

TOPICAL REVIEW

Recent advances in diffuse optical imaging

A P Gibson¹, J C Hebden¹ and S R Arridge²¹ Department of Medical Physics and Bioengineering, University College London, UK² Department of Computer Science, University College London, UK

Received 21 September 2004

Published 2 February 2005

Online at stacks.iop.org/PMB/50/R1

Abstract

We review the current state-of-the-art of diffuse optical imaging, which is an emerging technique for functional imaging of biological tissue. It involves generating images using measurements of visible or near-infrared light scattered across large (greater than several centimetres) thicknesses of tissue. We discuss recent advances in experimental methods and instrumentation, and examine new theoretical techniques applied to modelling and image reconstruction. We review recent work on *in vivo* applications including imaging the breast and brain, and examine future challenges.

1. Introduction

1.1. Diffuse optical imaging

Visible light and near-infrared (NIR) light interact with biological tissue predominantly by absorption and elastic scattering. There are several physiologically interesting molecules which have characteristic absorption spectra at these wavelengths. In particular, the spectra of oxy-haemoglobin (HbO) and deoxy-haemoglobin (HHb) differ markedly, as do the oxygenation-dependent spectra of cytochrome oxidase. Haemoglobin provides an indicator of blood volume and oxygenation, whereas the cytochrome enzymes indicate tissue oxygenation.

Unfortunately, while most of the physiological information is contained in the absorption coefficient (the number of absorption events per unit length, μ_a), the scatter coefficient (the number of scattering events per unit length, μ_s) in tissue is generally considerably larger, so that signals measured over distances of a few millimetres or larger are dominated by diffuse light. The physics of light transport in tissue has been explained in a number of recent review articles, for example Boas *et al* (2001a), Schweiger *et al* (2003) and Dunsby and French (2003), and will not be covered in detail here.

The different absorption spectra of HbO and HHb are routinely exploited in physiological monitoring techniques such as pulse oximetry and near-infrared spectroscopy (NIRS). Diffuse optical imaging techniques aim to process this information further and produce spatially resolved images. These images may display the specific absorption and scattering properties of the tissue, or physiological parameters such as blood volume and oxygenation. Diffuse

optical imaging generally falls into one of two categories: topography or tomography. The distinction between these two techniques has become somewhat blurred, but we use the term optical *topography* when referring to methods which produce two-dimensional (2D) images of a plane parallel to the sources and detectors with limited depth information, and use optical *tomography* to describe techniques which generate full three-dimensional (3D) images from measurements taken from sources and detectors widely spaced over the surface of the object.

1.2. Progress since 1997

In 1997, we published two reviews of ‘optical imaging in medicine’ in *Physics in Medicine and Biology* (Hebden *et al* 1997, Arridge and Hebden 1997) which summarized the state-of-the-art of the field of medical optical imaging at that time. The first review (Hebden *et al* 1997) examined instrumentation and experimental techniques, while the second review discussed modelling light transport in tissues and theoretical approaches to image reconstruction (Arridge and Hebden 1997). The focus of much of the experimental research at that time was on measuring and identifying minimally scattered photons, which (it was correctly concluded) cannot be applied to tissues more than a few millimetres thick. Improvement in spatial resolution was identified as a concern for diffuse optical imaging, and the potential for functional (and rapid) imaging of tissues (and of the brain in particular) was just beginning to be realised.

In this review, we examine the progress which has been made in diffuse optical imaging since the publication of the 1997 reviews. Recent advances in the field have largely focussed on the transfer of techniques from the laboratory to the clinic, and have led to the development of a broad variety of diagnostic applications, in particular imaging of the female breast and the adult and infant brain. While impressive, the progress has been evolutionary rather than revolutionary, although certain technological advances, in particular laser diodes and fast desktop PCs, have enabled progress to have been more rapid than would otherwise have been the case.

2. Experimental techniques

2.1. Detection of minimally scattered photons

It was recognized early in the history of optical imaging that photons which have been scattered a small number of times carry more spatial information than diffusive photons. Furthermore, if measurements could be made of minimally scattered photons, images could be reconstructed using the Radon transform as in x-ray CT, avoiding most of the difficulties associated with diffuse optical image reconstruction. Methods which can isolate minimally scattered photons from the diffusely scattered background, such as collimated detection, coherent techniques and time-gating were reviewed in detail by Hebden *et al* (1997). However, the fraction of minimally scattered photons transmitted across large (greater than several centimetres) thicknesses of tissue is immeasurably small, making this approach unsuitable for medical imaging. The length scale over which a collimated beam effectively becomes diffuse is known as the transport scattering length, which is about 1 mm in most biological tissues at NIR wavelengths. The transport scattering length is equal to the reciprocal of the transport scatter coefficient μ'_s , which is defined as $\mu'_s = (1 - g)\mu_s$, where μ_s is the scatter coefficient and g is the mean cosine of the scattering phase function.

Diffuse optical tomography can be contrasted with optical coherence tomography (OCT), which is a rapidly developing medical imaging modality, particularly in the area

of ophthalmology. It is a range-gating technique which exploits the coherent properties of back-reflected light to generate very high spatial and temporal resolution images of tissues with a penetration depth of a few millimetres (Boppart 2003, Fercher *et al* 2003, Fujimoto 2003).

Recently, the emphasis of research in medical imaging with diffuse light has moved away from the pursuit of high (\sim mm) spatial resolution and towards functional imaging. It is widely appreciated that diffuse optical imaging can never compete in terms of spatial resolution with anatomical imaging techniques (e.g. x-radiography, ultrasound and magnetic resonance imaging (MRI)), but offers several distinct advantages in terms of sensitivity to functional changes, safety, cost and use at the bedside. In the following sections, we review the alternative technological approaches currently being pursued, and discuss their relative merits and disadvantages.

2.2. Continuous wave systems

Measurements of the intensity of light transmitted between two points on the surface of tissue are not only relatively straightforward and inexpensive to obtain, but also contain a remarkable amount of useful information, as demonstrated by the clinical successes of NIRS (Obrig and Villringer 2003). So-called continuous wave (CW) systems require a source that either emits at a constant intensity, or is modulated at a low (a few kHz) frequency in order to exploit the significant improvements in sensitivity available from phase-locked detection techniques. CW sources have been used to investigate the head, testes and breast by viewing light which has been transmitted through the body since at least as far back as the early nineteenth century (Bright 1831, Curling 1843, Cutler 1929). CW transillumination of the breast (or ‘diaphanography’) received a brief revival of interest during the 1970s and 1980s with the introduction of NIR sources and detectors, but no significant clinical utility was demonstrated (Hebden and Delpy 1997).

Probably the most highly developed application of CW imaging technology is the study of haemodynamic and oxygenation changes in superficial tissues, and of the outer (cortical) regions of the brain in particular using optical topography. This typically involves acquiring multiple measurements of diffuse reflectance at small source–detector separations over a large area of tissue simultaneously or in rapid succession (see section 4.1). By keeping the separation small, measured signals are relatively high and therefore may be acquired quickly, enabling haemodynamic changes with characteristic responses as fast as a few tens of milliseconds to be studied. Thus, optical topography of the cortex represents a mapping technique analogous to electro-encephalography (EEG), which is sensitive to electrical activity in the cortex.

Recent technological advances have led to the development of arrays of individual sources and detectors which can be coupled to the head using flexible pads held in direct contact with the scalp. The availability of low-cost, high-power (several mW) and narrow bandwidth (less than a few nanometres) laser diodes over a broad range of NIR wavelengths have made them the popular choice of source for most optical imaging applications. The detector selected for a given application will depend on issues such as the desired sensitivity, stability and dynamic range, as well as more practical concerns such as size and cost. A variety of semiconductor photodiodes is available, usually offering very good dynamic range at low cost. Avalanche photodiodes (APDs) are generally the most sensitive of the semiconductor detectors. However, for optimum sensitivity, photomultipliers (PMTs) are required, which can provide single-photon counting performance, although with a more limited dynamic range and at significantly greater cost. A thorough review of detection methods is given by Knoll (1999).

The number of distinct sources or detectors required can be reduced by switching components sequentially to different optical fibres within the array (known as multiplexing), at the expense of reduced temporal resolution. Most current systems use multiple detectors to record signals continuously in parallel, while sources are either activated sequentially, or are intensity-modulated at different frequencies simultaneously. In the latter case, detected signals from specific sources are isolated either by using lock-in amplifiers (Yamashita *et al* 1999) or by Fourier transformation and appropriate filtration (Franceschini *et al* 2003, Everdell *et al* 2004). The former technique is used by the first commercial optical topography system, the Hitachi ETG-100 system. It consists of eight laser diodes at 780 nm and eight laser diodes at 830 nm, each modulated at a different frequency between 1 and 8.7 kHz (Yamashita *et al* 1999). The sources are coupled in pairs to eight distinct positions on the subject, while light is detected at eight further positions using APDs. An array of 48 lock-in amplifiers is used to sample 24 distinct source–detector combinations at two wavelengths, and thus Hitachi refer to this device as a 24-channel system. The system has been widely evaluated for brain imaging (see section 4.1) where the sources and detectors are distributed over one or two lobes of the brain (Yamashita *et al* 1999). A new model, the ETG-7000, is a 120-channel device which can image the entire adult cortex with 40 pairs of laser diodes and 40 APD detectors.

CW measurements have also been used for the considerably more challenging approach to imaging known as optical tomography, which involves generating a transverse slice or three-dimensional (3D) image (see section 3). Adequate sensitivity to deep tissues requires measurements at large source–detector separations, and consequently transmitted light must be integrated over periods of several seconds per source in order to obtain adequate signal. While this largely prohibits the analysis of short, isolated haemodynamic events, Schmitz *et al* (2002) have demonstrated a CW tomography system which uses gating and averaging of the detected signals to reveal cyclic haemodynamic changes (Barbour *et al* 2004). Their DYNOT (DYNAMIC Near-Infrared Optical Tomography) system is currently marketed commercially by NIRx Medical Technologies (USA).

During the late 1990s, Philips Research Laboratories (Netherlands) began evaluating a breast tomography system based on CW measurements and a simple back-projection algorithm (Colak *et al* 1999). The patient lay on a bed with her breast suspended within a conical chamber filled with a tissue-like scattering liquid. This approach had the very attractive benefit of eliminating the variability in surface coupling. The clinical performance of the Philips system was lower than desired, partly because of the inability of CW imaging to distinguish between internal absorbing and scattering properties (Arridge and Lionheart 1998). Similar commercial systems based on CW measurements have been developed by Imaging Diagnostic Systems Inc. (Grable *et al* 2004), see figure 1, and Advanced Research Technologies Inc. (Hawrysz and Sevick-Muraca 2000).

There are a number of disadvantages associated with CW imaging using absolute measurements of intensity:

- Intensity measurements are far more sensitive to the optical properties of tissues at or immediately below the surface than to the properties of localized regions deeper within the tissue. This is due to the characteristic ‘banana’ shape of the volume of tissue over which the measurement is sensitive (known as the photon measurement density function or PMDF), which is narrow near the source and detector and very broad in the middle (Arridge 1995, Arridge and Schweiger 1995).
- The detected intensity is highly dependent on surface coupling. For example, an optical fibre moved slightly or pressed more or less firmly against the skin can result in a very large change in the measurement. The presence of hair or local variation in skin colour can also have a major influence on intensity measurements. Although means of calibrating for



Figure 1. Imaging Diagnostic System Inc.'s computed tomography laser breast imaging system. See www.imds.com for more details.

variable surface coupling have been implemented (see section 3.4.6), NIRS and imaging using CW sources have largely focussed on recording *differences* in intensity, acquired over a period short enough so that the unknown coupling can be assumed to have remained constant.

- Measurements of intensity alone at a single wavelength are unable to distinguish between the effects of absorption and scatter (Arridge and Lionheart 1998).

Alternative types of measurements have been explored in order to circumvent some of these problems inherent in CW data. The techniques which have demonstrated the most promise for imaging through larger thicknesses of tissue are those based on the temporal measurement of transmitted radiation, or an equivalent measurement in the frequency domain. These are now reviewed separately in the following two sections.

2.3. Time-domain systems

The temporal distribution of photons produced when a short duration (a few picoseconds) pulse of light is transmitted through a highly scattering medium is known as the temporal point spread function (TPSF). After travelling through several centimetres of soft tissue, the TPSF will extend over several nanoseconds. Early technical validation studies, performed using laboratory picosecond lasers and a variety of sophisticated and expensive detector systems, such as streak cameras, were discussed in the 1997 review (Hebden *et al* 1997). Since then, advances in time-correlated single-photon counting (TCSPC) hardware and pulsed laser diodes have significantly reduced the cost and complexity of time-resolved measurement, and facilitated the development of multi-detector systems. TCSPC involves correlating the arrival time of a detected photon with the sampling of a known variable analogue signal. The difference between samples resulting from a detected photon and that from an external reference (derived directly from the source) provides a measurement of the photon flight time. An example of this technology is the time-to-amplitude converter (TAC). The technique generally requires a photon counting photomultiplier tube (PMT) detector. Maximizing temporal resolution requires a PMT with a minimum transient time spread (TTS)

of photoelectrons across the tube. PMTs with a TTS of 150–200 ps are available, but for a significantly shorter TTS (<50 ps) it is necessary to employ a microchannel-plate PMT (for examples, see www.hamamatsu.com). To date, the application of time-resolved measurement to diffuse optical imaging has involved two distinct approaches:

- A *transillumination* technique in which sources and detectors are arranged on opposite sides of a slab of tissue. Typically a single source and detector, aligned along a common axis, are scanned in two dimensions across each surface, and a single-projection image is produced directly. The approach was used in the first demonstration of 2D time-resolved imaging of tissue-like media by Hebden *et al* (1991), and the slab imaging geometry has been adopted for several breast imaging systems (Ntziachristos *et al* 1998, Grosenick *et al* 1999, Pifferi *et al* 2003), described in more detail in section 4.3. An array of sources or detectors is often used so that off-axis measurements are also available, which provides a degree of depth information sufficient for a 3D image reconstruction (Ntziachristos *et al* 1998, Grosenick *et al* 2004b).
- A *tomographic* approach to imaging, which involves placing sources and detectors over the available surface of the tissue in order to sample multiple lines-of-sight across the entire volume either simultaneously or successively. Images are then reconstructed using techniques such as those described in section 3.

Early applications of time-domain measurements used time-gating to identify those photons which first emerge from the tissue, which are assumed to have travelled the shortest distance and therefore be least scattered. This approach is, however, limited by the number of available photons with sufficiently short flight times. Experiments by Hebden and Delpy (1994) indicated that a degree of high-resolution information is encoded into the shape of the TPSF, which can be extracted if the TPSF is measured sufficiently accurately. Time-gating techniques have also been developed which discriminate between late arrival photons which are predominantly affected by absorption, and early arrival photons which depend on both absorption and scatter (Grosenick *et al* 2003). More recently, Selb *et al* (2004) showed that time-gating can be used to provide additional depth resolution compared with CW measurements alone by rejecting light from superficial tissues.

Time-resolved measurements were first applied to clinical optical tomography by researchers at Stanford University (Benaron *et al* 2000, Hintz *et al* 2001), who developed an imaging system which was used to measure photon flight times between points on a newborn infant's head (see section 4.2). However, since only a single solid-state detector was used, transmitted light between each combination of source and detector position was recorded sequentially, resulting in scan times of between two and six hours. Much faster scan times are achievable by using multiple detectors, as demonstrated by the 32-channel time-resolved system developed at University College London (UCL) (Schmidt *et al* 2000), and a 64-channel time-resolved imaging system built by Shimadzu Corporation in Japan (Eda *et al* 1999).

The UCL system is based on TCSPC technology and a dual-wavelength fibre laser. The laser provides interlaced trains of picosecond pulses at 780 nm and 815 nm which are coupled to the surface of the subject via a 32-way optical-fibre switch. Transmitted light is collected simultaneously by 32 detector fibre bundles, which deliver the light to four 8-anode microchannel-plate PMTs via 32 variable optical attenuators, which ensure that the intensity of detected light does not exceed the maximum photon counting rate of around 2.5×10^6 photons per second. The arrival time of each detected photon is measured with respect to a laser-generated reference signal, and TPSFs are accumulated.

2.4. Frequency-domain systems

A time-domain measurement can be equivalently expressed in the frequency domain. Some researchers have developed imaging systems which acquire frequency-domain data directly using a source that is amplitude modulated at a high frequency (a few hundred MHz), and measuring the reduction in amplitude and phase shift of the transmitted signal. While time-resolved measurements have the advantage of acquiring information at all frequencies simultaneously, frequency-domain systems can employ light sources and detectors which are significantly less expensive than those required for time-resolved systems.

The science and technology of phase measurement for NIRS and imaging has been comprehensively reviewed by Chance *et al* (1998b). Systems require a radio-frequency (RF, typically a few hundred MHz) oscillator to drive a suitable laser diode and to provide a reference signal for the phase measurement device which receives the detected signal from an appropriate high-bandwidth detector (e.g. PMT or APD, depending on the desired sensitivity). Heterodyning is commonly performed to convert the RF to a few kHz prior to phase detection. The detected signal is digitized over an appropriate period of time, and phase and amplitude are computed.

The transillumination and tomographic approaches described in section 2.3 for time-resolved systems are equally applicable for frequency-domain devices, and both have been widely explored. In the mid-1990s two major companies in Germany reported development of breast imaging systems based on frequency-domain measurement of transmitted light. These prototypes, constructed by Carl Zeiss (Kaschke *et al* 1994, Moesta *et al* 1996) and by Siemens (Götz *et al* 1998), both involved rectilinear scanning of a single source–detector pair over opposite surfaces of a compressed breast, resulting in single-projection images at multiple NIR wavelengths. Unfortunately, the performance of both systems during quite extensive trials fell below that required of a method of screening for breast cancer, although various improvements to the Carl Zeiss system and their reconstruction method have since been implemented (Franceschini *et al* 1997, Fantini *et al* 1998).

As summarized in section 4, a variety of frequency-domain systems have been developed for both optical topography (Danen *et al* 1998, Franceschini *et al* 2000) and optical tomography (Pogue *et al* 2001). Culver *et al* (2003a) have built a hybrid CW/frequency-domain device for optical tomography which combines the benefits of speed and low cost of CW measurements with the ability to separate scatter and absorption available from the amplitude and phase of frequency-domain data. The system employs four amplitude-modulated laser diodes operating at different wavelengths (690 nm, 750 nm, 786 nm and 830 nm) which are rapidly switched between 45 optical fibres on a 9×5 array. The array is positioned against one side of a compressed breast, while light emerging on the opposite side is focused onto a CCD camera. Meanwhile, diffusely reflected light is detected simultaneously by APDs via nine fibres interlaced among the source fibres. The amplitude and phase of the APD signals are determined using a homodyne technique.

2.5. Comparison of time-domain and frequency-domain systems

The relative advantages and disadvantages of frequency-domain optical imaging systems compared to time-domain systems have been subject to debate for more than ten years. Frequency-domain systems are relatively inexpensive, easy to develop and use, and can provide very fast temporal sampling (up to 50 Hz). Time-domain systems, on the other hand, tend to use photon counting detectors which are slow but highly sensitive. Hence, frequency-domain systems are well suited to acquiring measurements quickly and at relatively high

detected intensities (such as for topography applications). However, when imaging across large (>6 cm) thicknesses the light intensity is very low, possibly only a few photons per second, and can only be detected using the powerful pulsed laser sources and photon counting techniques incorporated into time-resolved systems.

The information content in a TPSF is inevitably greater than that in a single phase and amplitude measurement at one source frequency, but the magnitude of this benefit has yet to be thoroughly explored. The frequency content of the TPSF extends to several GHz, and while in principle a frequency-domain system could be designed to acquire this information, it is not yet possible to modulate high-intensity sources at such high frequencies. The intensity and mean photon flight time calculated from the TPSF are almost equivalent to the amplitude and phase of a frequency-domain system (Arridge *et al* 1992). Other data types calculated from the TPSF such as variance, skew and the Laplace transform can provide enhanced separation between μ_a and μ'_s (Schweiger and Arridge 1999a), but may be more sensitive to noise. These additional data types have no simple equivalent in the frequency domain. Other approaches, such as time-gating to distinguish between μ_a and μ'_s (Grosenick *et al* 2003) or to provide depth discrimination (Selb *et al* 2004) also demonstrate the additional information available in the TPSF.

Practical optical measurements, particularly in the hospital, are commonly contaminated by constant (or temporally uncorrelated) background illumination. Frequency-domain systems are able to reject uncorrelated signals (but not the uncorrelated noise associated with these signals) by the use of lock-in amplifiers, while time-domain systems reject photons which reach the detector outside a finite temporal window. However, frequency-domain systems are unable to identify unwanted light which is temporally correlated with the measurement, such as light which has leaked around the object being imaged. In the time-domain, inspection of the TPSF can enable these contaminated measurements to be rejected (Hebden *et al* 2004b).

2.6. Selection of optimal wavelength

The choice of wavelengths to use for NIR studies is a complex one. The 'NIR window' used for tissue optics is bounded roughly between 650 nm and 850 nm. At lower wavelengths, absorption by haemoglobin limits penetration in tissue, while at higher wavelengths, absorption by water dominates. NIRS studies of the brain have typically employed wavelengths either side of the isobestic point of haemoglobin at 800 nm, where the specific extinction coefficients of HbO and HHb are equal. The actual wavelengths used for a given study are often determined in an *ad hoc* way and are often dictated by the availability of appropriate light sources (Cope 1991). Recently, Yamashita *et al* (2001) Strangman *et al* (2003) and Boas *et al* (2004a) have shown experimentally and theoretically that a pair of wavelengths at 660–760 nm and 830 nm provides superior separation between HHb and HbO than the more commonly used 780 and 830 nm.

Pifferi *et al* (2003) and Taroni *et al* (2004a) have investigated the additional information obtained by using a wider range of wavelengths. They used four wavelengths (683 nm, 785 nm, 912 nm and 975 nm) to image the breast, with the wavelengths selected empirically to optimize distinction between HbO, HHb, water and lipids. They also found that using four shorter wavelengths (637 nm, 656 nm, 683 nm and 785 nm) improved the distinction between tumours and cysts.

The first systematic evaluation of the optimal wavelengths for NIR imaging was carried out by Corlu *et al* (2003) who determined the wavelengths which minimized cross-talk between chromophores by maximizing the uniqueness with which different chromophores can be distinguished. They simulated spatially varying distributions of HbO, HHb, water

and scattering coefficient, and determined the four wavelengths which minimized cross-talk between the chromophores. These did not correlate with the wavelengths which had been assumed to be optimal for NIRS studies. Such theoretical studies are of growing importance as advances in laser diode technology allow a much greater choice of wavelengths. This work also introduced the concept of reconstructing for chromophore concentration directly, rather than the more usual method of post-processing images generated at different wavelengths.

Uludag *et al* (2004) used both theoretical and experimental methods to investigate the way in which cross-talk between calculated HHb and HbO concentrations ($[HHb]$ and $[HbO]$) from dual-wavelength measurements is affected by noise and error in the measurement. Their results agreed with those of Yamashita *et al* (2001) and Strangman *et al* (2003), i.e. one of the selected wavelengths should be much shorter than 780 nm. They also showed that non-optimal wavelengths can lead to cross-talk which not only reduces the quantitative accuracy with which the changes can be determined but also changes the *shape* of the time-course of the signal.

2.7. Other approaches

The predominant factor which reduces the image quality in diffuse optical imaging is scatter, and many of the advances in instrumentation, theory and experimental techniques have been designed to reduce its effect. We will briefly mention two techniques which have been developed to improve the spatial resolution of diffuse optical imaging by combining the functional sensitivity of NIR measurements with the spatial resolution of ultrasound.

Ultrasound is an acoustic wave which can be used to modulate the amplitude of light travelling through a compressible object. This was exploited by Wang *et al* (1995), who used a focused ultrasound beam to modulate single channel optical measurements recorded across a cuvette. The amplitude of the modulated optical signal carried information about the optical properties at the focus of the ultrasound beam and was used to produce high-resolution images of the optical properties. Li *et al* (2002) developed the technique further by imaging the output field with a CCD camera and analysing the laser speckle, which correlated with the ultrasonic modulation. They successfully imaged objects embedded in 25 mm thickness of tissue.

Photoacoustic imaging offers a further approach to combining the advantages of ultrasound and optical methods. When NIR light passes through tissue, it is absorbed, heating the tissue. The heated tissue expands and produces an acoustic wave which can be measured using conventional ultrasound detectors at the surface. An image of the sources of the ultrasound signal reveals the regions of highest optical absorption within the tissue, with the spatial resolution of ultrasound. Wang *et al* (2003) have used photoacoustic techniques to produce anatomical and functional images of the intact rat brain with a spatial resolution of 200 μm .

3. Modelling and reconstruction

3.1. Background

The 1997 review of modelling and image reconstruction techniques (Arridge and Hebden 1997) is still a useful introduction to the basic theoretical concepts. Progress since 1997 has largely focused on developing more realistic and efficient models of light transport in tissue, and on solving the ill-posed inverse problem in an increasingly rigorous way. In particular, it is becoming increasingly common to include prior information of the anatomy and optical properties of tissue in both the modelling and the image reconstruction.

Three processes are required to reconstruct an optical image. First, the transport of light in tissue must be modelled. Second, this model must be used to predict the distribution of light in the object under examination. This stage, the *forward problem*, allows the measurements to be simulated from the model, and generates (explicitly or implicitly) a sensitivity matrix (the Jacobian of the forward mapping) which relates the measurements to the internal optical properties. Finally, the image is reconstructed by inverting the Jacobian and solving the *inverse problem*. In x-ray CT, scatter is minimal, so the forward problem becomes a series of integrals along lines connecting the sources and detectors (a Radon transform), and the inverse problem is linear and well posed. In optical imaging, however, scatter is dominant, meaning that the forward problem becomes a series of integrals over the entire volume. Each measurement is therefore sensitive to the whole volume, meaning that the inverse problem is ill-posed and underdetermined and that complex, computer-intensive reconstruction techniques are required. For recent reviews of image reconstruction in optical imaging, see Arridge (1999), Kohlemainen (2001) and Schweiger *et al* (2003).

It should be noted that similar issues are being addressed in electrical impedance tomography (EIT), which is a related medical imaging technique in which surface measurements of electrical impedance are used to reconstruct volume images of tissue conductivity (Metherall *et al* 1996, Borcea 2002, Lionheart 2004).

3.2. Modelling light transport in tissue

Before image reconstruction can be attempted, a model of photon transport in tissue is required. For diffuse optical imaging, the diffusion equation, in which the propagation of light is assumed to be isotropic, is commonly used. In this section, we discuss the derivation of the diffusion equation from the radiative transport equation. Arridge (1999) provides a more detailed review.

A full description of light propagation in tissue is provided by the radiative transport equation (RTE; equation (1)). This is a conservation equation which states that the radiance (the number of photons per unit volume), $\phi(r, \hat{s}, t)$, for photons travelling from point r in direction \hat{s} at time t is equal to the sum of all the mechanisms which increase ϕ minus those effects which reduce it. Equation (1) shows the time-domain RTE. The RTE in the frequency-domain is obtained by replacing $\partial/\partial t$ by $i\omega$.

$$\left(\frac{1}{c} \frac{\partial}{\partial t} + \hat{s} \cdot \nabla + \mu_{\text{tr}}(r) \right) \phi(r, \hat{s}, t) = \mu_s(r) \int_{S^{n-1}} \Theta(\hat{s}, \hat{s}') \phi(r, \hat{s}', t) d\hat{s}' + q(r, \hat{s}, t). \quad (1)$$

In (1), $\Theta(\hat{s}, \hat{s}')$ is the scatter phase function, which gives the probability of a photon scattering from direction \hat{s} to \hat{s}' , $\mu_{\text{tr}} = \mu_a + \mu_s$ and $q(r, \hat{s}, t)$ is the light source at r at time t travelling in direction \hat{s} . For clarity, we use the same symbols as Arridge (1999).

The RTE is an approximation to Maxwell's equations and has been used successfully to model light transport in diffusive media, turbulence in the earth's atmosphere, and neutron transport. However, it does not include wave effects, so the wavelength must be much smaller than the dimensions of the object under study. It also requires the refractive index to be constant in the medium, although extensions for spatially varying refractive index have been derived (Ferwerda 1999, Marti-Lopez *et al* 2003, Tualle and Tinetti 2003). Unfortunately, to solve for the properties of the light field at all points in a large 3D volume, as is required in optical tomography, the RTE is extremely computationally expensive and simpler models are generally sought. Kim and Keller (2003) recommend the use of a modified Fokker–Planck equation as an approximation to the RTE where scatter is strongly forward-biased.

Three variables in the RTE depend on direction \hat{s} : the specific intensity ϕ , the phase function Θ and the source term q . If these are expanded into spherical harmonics, we obtain an infinite series of equations which approximate to the RTE. The P_N approximation is obtained by taking the first N spherical harmonics, which gives $(N + 1)^2$ coupled partial differential equations. As N increases, the P_N approximation models the RTE more accurately, but with increasing computational requirements (Aydin *et al* 2002).

If we now take the P_1 approximation and assume that the phase function $\Theta(\hat{s}, \hat{s}')$ is independent of the absolute angle, i.e. $\Theta = \Theta(\hat{s} \cdot \hat{s}')$, that the photon flux changes slowly and that all sources are isotropic, we obtain the diffusion equation (2),

$$-\nabla \cdot \kappa(r) \nabla \Phi(r, t) + \mu_a \Phi(r, t) + \frac{1}{c} \frac{\partial \Phi(r, t)}{\partial t} = q_0(r, t), \quad (2)$$

where photon density $\Phi(r, t) = \int_{S^{n-1}} \phi(r, \hat{s}, t) d\hat{s}'$, and the diffusion coefficient $\kappa = 1/3(\mu_a + \mu_s')$.

The diffusion equation (2) has been widely and successfully used to model light transport in tissue, although it is necessary to assume that light propagates diffusively. This is generally the case in bulk tissue but the assumption breaks down near the source, near the surface, near internal boundaries, in anisotropic tissues, and in regions of either high absorption or low scatter. In these situations, higher order approximations to the RTE may be required.

3.3. Forward problem

3.3.1. Analytical modelling techniques. Green's functions provide a method for modelling the diffusion equation or the RTE analytically. The Green's function is the solution when the source is a spatial and temporal δ -function, from which solutions for extended sources can be derived by convolution. Unfortunately, solutions only exist for simple homogeneous objects (Arridge *et al* 1992) or media which include a single spherical perturbation (Boas *et al* 1994), although the range of solutions is being extended to more complex geometries such as layered slabs (Martelli *et al* 2002).

A number of workers have extended this type of approach. Kim (Kim and Ishimaru 1998, Kim 2004) has devised a method for calculating the Green's function as an expansion into plane-wave solutions, which allows analytical solutions for the diffusion equation or the RTE to be derived. Ripoll *et al* (2001) have advocated the use of the Kirchhoff approximation, which models the Green's function between two points in a medium of arbitrary geometry as a sum of the infinite space Green's function plus other Green's functions calculated for diffusive waves which are multiply reflected off the boundary. It can be used alone, or to improve the accuracy of existing modelling techniques. Green's function techniques are now commonly used to solve the forward problem for image reconstruction, particularly for fast imaging techniques where the geometry can be approximated as a slab or an infinite half-space, such as for optical topography (Culver *et al* 2003c, Li *et al* 2004).

Spinelli *et al* (2003) have developed a perturbation approach first introduced by Arridge (1995) in which the optical properties are modelled by a Green's function for a slab representing the homogeneous background, with an additional perturbation term representing a spherical insertion. It is well suited to analysing transmission data measured across a compressed breast with a single, isolated lesion (Torricelli *et al* 2003).

3.3.2. Statistical modelling techniques. Statistical (or stochastic) modelling techniques model individual photon trajectories and have the advantage that the Poisson error is incorporated into the model in a natural and elegant way. The most commonly used statistical technique in diffuse optics, and that which is often regarded as the 'gold standard' to which

other techniques are compared, is the Monte Carlo method. The geometry of the model is defined in terms of μ_a , μ_s , $\Theta(\hat{s}, \hat{s}')$ and the refractive index, and the trajectories of photons, or packets of photons, are followed until they either escape from the object under study or are absorbed. By continuing until the required counting statistics are obtained, data with arbitrarily low statistical errors can be simulated. In optical imaging, Monte Carlo techniques are commonly used to calculate light propagation in non-diffusive domains where the diffusion approximation does not hold (Boas *et al* 2002, Okada and Delpy 2003, Hayashi *et al* 2003), or to validate results obtained using other, faster, methods (Schweiger *et al* 1995, Chernomordik *et al* 2002b, Dehghani *et al* 2003a).

Random walk theory provides a distinct approach in which photon transport is modelled as a series of steps on a discrete cubic lattice. The time steps may be discrete or continuous (Weiss *et al* 1998). Random walk theory is particularly suited to modelling time-domain measurements (Chernomordik *et al* 2000) and has been used, for example, to determine the time spent by photons in a scattering inclusion (Chernomordik *et al* 2002a) and to quantify the optical properties of a breast tumour (Chernomordik *et al* 2002b). Recently, an extension to the technique has been developed for modelling media with anisotropic optical properties (see section 3.3.6), maintaining the cubic lattice but allowing the transition properties along different axes to differ (Dagdug *et al* 2003). Similarly, Carminati *et al* (2004) have developed a more general method based on random walk theory which allows the transition from single-scattering to diffusive regimes to be explored.

3.3.3. Numerical modelling techniques. Numerical techniques are required if more complex geometries are to be modelled. The natural choice for representing the inhomogeneous distribution of optical properties in an arbitrary geometry is the finite element method (FEM) which was first introduced into optical tomography by Arridge *et al* (1993). The method is explained in detail by Arridge and Schweiger (1995), Arridge (1999) and Arridge *et al* (2000a). FEM has become the method of choice for modelling complex inhomogeneous domains in optical imaging (Bluestone *et al* 2001, Dehghani *et al* 2003b), although the finite difference method (FDM) (Culver *et al* 2003a, Hielscher *et al* 2004), finite volume method (FVM) (Ren *et al* 2004) and boundary element method (BEM) (Ripoll and Ntziachristos 2003, Heino *et al* 2003) have been used in more specialized applications.

The finite element method requires that the reconstruction domain be divided into a finite element mesh. In principle, this is a completely general technique which can be applied to any geometry. In practice, however, it is difficult to create a finite element mesh of irregular objects with complex internal structure, and the development of robust, efficient 3D meshing techniques is still the subject of active research. A particular challenge is meshing the head, while respecting the convoluted internal boundaries of the scalp, skull, cerebrospinal fluid (CSF), grey matter and white matter derived from a segmented MRI image. Inclusion of such anatomical details has been shown to improve the quality of reconstructed images in EIT (Bagshaw *et al* 2003), although generating the 3D finite element mesh was difficult and time-consuming (Bayford *et al* 2001, Lionheart 2004). The use of realistic finite element meshes in optical imaging has progressed from 2D models of internal structure taken from segmented MR images of the head and breast (Schweiger and Arridge 1999b, Brooksby *et al* 2003), through 3D finite element meshes with complex surface shape but no internal structure (Bluestone *et al* 2001, Gibson *et al* 2003, Dehghani *et al* 2004), to a recent report by Schweiger *et al* (2003) of simulations from 3D finite element meshes of the breast and head with anatomically realistic internal structure. A further complication is the consideration that optimal computational efficiency requires a finite element mesh which can represent the internal field adequately whilst using the smallest possible number of elements. One approach is to adaptively refine

the mesh, placing more elements where the field changes most rapidly (Molinari *et al* 2002, Joshi *et al* 2004). Another approach, which is suited to modelling a segmented volume taken from MRI, is to resample the pixels in the MRI image onto a regular grid which can then be solved with FDM (Barnett *et al* 2003).

3.3.4. Use of prior information. Perhaps the most significant recent trend in optical imaging has been the inclusion of prior anatomical information into the forward problem, most commonly in the form of an anatomical MRI image. Prior information was first used in optical tomography reconstruction by Pogue and Paulsen (1998), and by Schweiger and Arridge (1999). The latter used a more sophisticated reconstruction procedure, which began by building a finite element mesh with four regions segmented from an MR image. They smoothed the model to account for gradual transitions between regions and generated simulated data, to which noise was added. They then used a two-step reconstruction process in which the optical properties of the regions were reconstructed first, followed by a full reconstruction onto the finite element mesh basis. The use of prior anatomical information was shown to improve the image quality in all cases. Ideally, the anatomical prior and the optical image should be acquired simultaneously so the two images are correctly registered. This impacts on the design of the image acquisition system and the experimental procedure and so these approaches are reviewed in the appropriate section on clinical applications below.

3.3.5. Non-diffusive regions. Light transport can be modelled adequately using the diffusion approximation in most biological tissues. Among the exceptions to this are tissue volumes which are smaller than a few scattering lengths, and regions where μ_a is comparable to or greater than μ'_s , such as the CSF which surrounds the brain and fills the central ventricles. These regimes are generally modelled using higher order approximations to the RTE.

It is generally too computationally expensive to solve the RTE fully in a practical reconstruction scheme. Instead, approximations are made such as the method of discrete ordinates, which solves the full RTE on a regular grid using FDM or FVM by quantizing the allowed directions of travel, \hat{s} . This makes the problem tractable but because only preferred angles of travel are allowed, there may be regions where light cannot reach. This is known as the *ray effect* and restricts the application of the method. The method of discrete ordinates was applied to optical imaging by Dorn (1998) and has been used successfully (Klose and Hielscher 1999, Ren *et al* 2004) for imaging small objects such as the finger (Hielscher *et al* 2004), and in fluorescence and molecular imaging of small animals (Klose *et al* 2004). Alternatively, the RTE can be solved using the P_N approximation (Aydin *et al* 2002) or by expansion into a rotated spherical harmonic basis (Markel 2004).

A different approach can be taken for modelling light transport in the head, where the healthy CSF is non-scattering (although brain injury may cause proteins and blood products to leak into the CSF, making it diffusive (Seehusen *et al* 2003)). If an anatomical MRI is available, then it is possible to segment the head into diffusive and non-diffusive regions. A coupled radiosity-diffusion model has been developed at UCL which models light transport in scattering regions using the diffusion model, and in clear regions using a visibility model which couples points on the void boundary which are mutually visible. The model has been applied to 2D (see figure 2) and some 3D geometries (Riley *et al* 2000), but it has not yet been applied to a 3D head-like model. A similar approach has been adopted by Schulz *et al* (2003, 2004) who use a coupled model for non-contact molecular imaging where the animal is modelled diffusively and the space between the optical fibres and the animal is modelled using a free-space propagation model. One disadvantage of the current implementation of the radiosity-diffusion model is that the boundary of the clear region must be known.

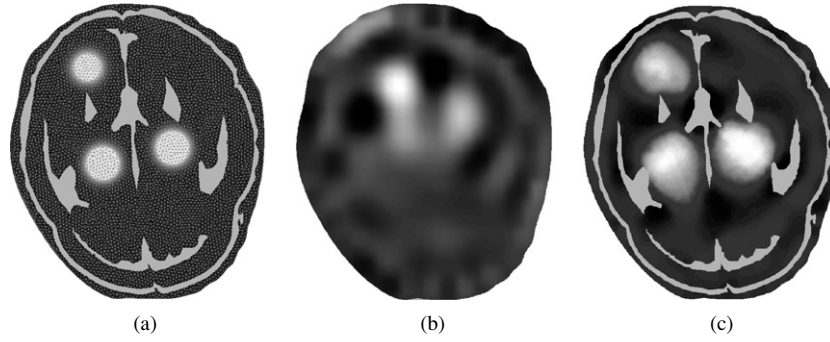


Figure 2. The effect of non-scattering regions on image reconstruction; (a) shows the 2D target mesh, segmented from an MR image of a neonatal head with the clear regions of CSF identified and three targets added with twice the background absorption; (b) is an image reconstructed using mean photon flight time data simulated from (a) assuming the domain is diffusive everywhere; (c) is a reconstruction, given prior information about the location of the clear regions, which are modelled using the radiosity-diffusion method.

3.3.6. Anisotropy. Another regime in which the diffusion approximation does not apply is that of anisotropic scattering. Certain tissues such as the skin, nervous tissue and muscle cells are anatomically anisotropic at the cellular level, and this leads to anisotropic scattering properties (Nickell *et al* 2000).

Heino and Somersalo (2002) derived a modified form of the diffusion equation in which the diffusion coefficient, $\kappa = \frac{1}{3(\mu_a + \mu_s[1-g])}$, is replaced by a diffusion tensor $\kappa = \frac{1}{3([\mu_a + \mu_s]1 - \mu_s S)}$, where S is (in 3D) a 3×3 matrix whose diagonal contains the anisotropic scattering coefficients. They make the anatomically realistic assumption that μ_a is isotropic everywhere and distinguish between knowing *a priori* the direction but not the strength of the scatter anisotropy (as may be obtained from MR diffusion tensor imaging (Le Bihan *et al* 2001)), and having full knowledge of both the direction and the strength of the anisotropy. Such prior information is required if the solution is to be unique. Statistical reconstructions of simulated data demonstrated that artefacts in μ_a will result if anisotropic μ'_s is not fully considered. They validated the results by comparison with a Monte Carlo model (Heino *et al* 2003).

Dagdug *et al* (2003) studied the same problem using a random walk formulation in which the transition probability is allowed to vary with direction. To date, this method only allows the direction of anisotropy to be parallel to the coordinate axes. The model has been shown to agree with time-resolved measurements on anisotropic phantoms (Hebden *et al* 2004a).

3.4. Image reconstruction

3.4.1. Linear image reconstruction. The forward problem, discussed above, involves calculating simulated data y (which may be CW, time-domain or frequency-domain data), given a forward operator F and knowledge of the sources q and internal optical properties x (which may include μ_a and μ'_s). The forward problem may therefore be formulated as

$$y = F(x). \quad (3)$$

To reconstruct an image, it is necessary to solve the inverse problem, which is to calculate the internal optical properties x , given data y and sources q (Arridge 1999):

$$x = F^{-1}(y). \quad (4)$$

This is a non-linear problem but it can be linearized if the actual optical properties x are close to an initial estimate x_0 and the measured data y are close to the simulated measurements y_0 . This is typically the case in difference imaging where measurements are taken before and after a small change in the optical properties. Then we can expand (3) about x_0 in a Taylor series,

$$y = y_0 + F'(x_0)(x - x_0) + F''(x_0)(x - x_0)^2 + \dots \quad (5)$$

where F' and F'' are the first- and second-order Fréchet derivatives of F , respectively. The Fréchet derivative is a linear integral operator mapping functions in the image space to functions in the data space. In some cases, such as in section 3.3.1, the kernel of the integral operator is known in terms of the Green's functions. This approach was taken by Boas *et al* (1994).

More generally, the forward problem can be solved by a numeric technique by representing the Fréchet derivatives F' and F'' by matrices \mathbf{J} (the Jacobian) and \mathbf{H} (the Hessian), respectively. Equation (5) can then be linearized by neglecting higher order terms and considering changes in the optical properties $\Delta x = x - x_0$ and data $\Delta y = y - y_0$ to give the linear problem (6):

$$\Delta y = \mathbf{J}\Delta x. \quad (6)$$

Linearizing the change in intensity in this way gives rise to the Born approximation; linearizing the change in log intensity instead is the Rytov approximation and may lead to improved images by reducing the dynamic range of y . Either way, image reconstruction consists of the problem of inverting the matrix \mathbf{J} , or some form of normalized \mathbf{J} . This may be large, underdetermined and ill-posed but standard matrix inversion methods can be used. These techniques differ in the way in which the matrix inversion is regularized to suppress the effect of measurement noise and modelling errors. Perhaps the most common techniques are truncated singular value decomposition, Tikhonov regularization and the algebraic reconstruction technique (ART) (Gaudette *et al* 2000). The Moore–Penrose inverse $\mathbf{J}^{-1} = \mathbf{J}^T(\mathbf{J}\mathbf{J}^T)^{-1}$ offers a more efficient inversion if \mathbf{J} is underdetermined and leads naturally to a Tikhonov-type formulation (7) where \mathbf{I} is the identity matrix and λ is a regularization parameter. \mathbf{J} itself is calculated from the forward model, most efficiently using the adjoint method of Arridge and Schweiger (1995). The linear inverse problem can then be expressed as

$$\Delta x = \mathbf{J}^T(\mathbf{J}\mathbf{J}^T + \lambda\mathbf{I})^{-1}\Delta y. \quad (7)$$

3.4.2. Non-linear image reconstruction. If the inverse problem cannot be assumed to be that of reconstructing the *difference* between two similar states, but is instead a reconstruction from a single acquisition to obtain *absolute* values of the optical properties, the linear approximation cannot be justified and the full non-linear problem must be solved. This is commonly the case in breast imaging (Dehghani *et al* 2003b), and in static imaging of the brain (Bluestone *et al* 2001, Hintz *et al* 2001, Hebden *et al* 2002). To solve the non-linear problem, we define an objective function ψ , which represents the difference between the measured data y and data which are simulated using the forward model $F(x)$. If \hat{x} is the distribution of optical parameters which minimizes ψ , then it is also the model which best fits the data, and is therefore taken to be the image. However, because the problem is ill-posed, it must be regularized, and can be expressed as

$$\psi = \|y - f(x)\|^2 + \alpha\|\Pi\|^2, \quad (8)$$

where α is a regularization parameter, and Π represents prior information. This may be very simple, for example $\Pi = \mathbf{I}$, in which case (8) becomes an iterative solution of (7). However, it is increasingly common for Π to include anatomical and other information, see section 3.4.3.

$\|\cdot\|^2$ represents the L2-norm and gives the least squares solution. Equation (8) can be extended to include the covariance of the data C_P and the covariance of the image C_Q as follows:

$$\psi = (y - f(x))^T C_P (y - f(x)) + \alpha (\Pi^T C_Q \Pi). \quad (9)$$

This approach gives a weighted least squares solution which reduces the influence of noise and cross-talk both in the data and in the image. Measuring C_P and C_Q may not be straightforward. Equation (9) is a non-linear minimization problem which is generally solved either by a Newton method such as the Levenberg–Marquardt algorithm, or by a gradient method such as conjugate gradients (Arridge 1999).

3.4.3. Uniqueness. No general uniqueness results exist for optical imaging, because of the range of different unknowns (μ_a , μ'_s , refractive index, coupling coefficients, anisotropy, geometry, etc) and the range of different measurables (time-domain or frequency-domain measurements or CW measurements of intensity alone). Some useful results do exist, however, to illustrate situations which may not yield unique solutions (Isakov 1993).

The first important uniqueness result directly relevant to the diffusion equation was derived by Arridge and Lionheart (1998) and developed further by Arridge (1999). They demonstrated that measurements of intensity alone cannot separate the effects of absorption and scatter. Furthermore, if the refractive index is also unknown, even frequency-domain or time-domain measurements are not sufficient for uniqueness, although Matchler (1999) showed that uniqueness may be restored if the underlying model is taken to be the P_1 approximation. The specific case of optical mammography using a slab geometry was analysed by Romanov and He (2000), who showed that if full time-domain data are available then reflection measurements (where the sources and detectors are on the same side of the slab) can uniquely determine a piecewise continuous distribution of either μ_a or μ'_s if the other parameter is given, but transmission measurements can distinguish μ_a and μ'_s if both are unknown. In an interesting application of uniqueness theory, Corlu *et al* (2003) used a uniqueness argument to determine which wavelengths gave the optimal separation between different chromophores in spectroscopic imaging, and to reconstruct directly for chromophore concentration.

Arridge and Lionheart (1998) illustrated their uniqueness result with an example of two distributions of μ_a and μ'_s which gave indistinguishable intensity data on the boundary, and Hoenders (1997) described a whole class of solutions which could not be distinguished from one another. More specifically, Schweiger and Arridge (1999a) plotted the objective function of the inverse problem against μ_a and μ'_s for a range of different data types extracted from the TPSF and showed that, although certain combinations of data types gave a well-behaved minimum, measurements of intensity alone gave an objective function with an extended minimum at approximately $\mu_a \mu'_s = \text{constant}$, suggesting that μ_a and μ'_s could not be separated.

However, as Hoenders (1997) points out, the existence of a solution to an inverse problem depends on more than just the uniqueness. It also depends on other issues including the quality of the data and the statistical behaviour of the problem. In particular, even if a problem is non-unique, it may be possible to distinguish between two identical data sets if appropriate prior information is available, whether it is used implicitly in the form of regularization or normalization of the Jacobian (Pei *et al* 2001, Xu *et al* 2002a), or explicitly. This may enable the theoretical results outlined above to be reconciled with experimental work by (Schmitz *et al* 2002) and (Pei *et al* 2001), and by (Jiang *et al* 2002) and (Xu *et al* 2002a) who have reconstructed images showing some separation between μ_a and μ'_s from intensity data alone. It remains to be seen how non-uniqueness affects reconstruction of

clinical images, where the potential for a reconstruction to converge to an incorrect solution may be unacceptable.

3.4.4. Use of prior information. Advances in modelling and reconstruction techniques cannot overcome the fact that diffuse optical imaging is a non-unique, ill-posed, underdetermined problem and that this puts a limit on the image quality, particularly the spatial resolution, which can be achieved. One way to improve the quality of the image reconstruction is to make maximum use of prior information, which can be obtained from anatomical imaging techniques or by considering the physics and the physiology of the problem. This reduces the effect of the ill-posedness by improving the accuracy of the model, and makes the problem better determined by allowing the small number of measurements which are obtained to be used in a more effective way. For example, Ntziachristos *et al* (2000) used an MR image of a breast to provide the location of a tumour *a priori*. Using this approach, the spatial resolution of the optical image effectively becomes that of the MR image. The reduction in quantitative accuracy due to the partial volume effect seen in optical images reconstructed without prior information does not occur, and truly quantitative images of the haemodynamic properties of the tumour can be obtained.

The most straightforward way to include prior information into the image reconstruction is to use an anatomically realistic forward model (section 3.3.3). This increases the accuracy of the forward model so that it can represent the measurements more precisely, thereby improving the image reconstruction. Further improvements can be made by including information about the covariance of the data C_P , and of the image C_Q , as in (9). The diagonal of C_P is simply the variance of each measurement, and gives an indication of the reliability of that measurement. Off-diagonal elements are the covariance between each pair of measurements and give an indication of the interdependence between measurements. Introducing C_P into (9) transforms the fit between the data and the model into a basis where all measurements are independent. C_Q contains information about the predicted smoothness of the image.

Prior knowledge of the anatomy can also be incorporated into the inverse problem. In the example of a breast tumour given above, the change in optical properties is assumed to come from either a region of interest defined from anatomy (Ntziachristos *et al* 2002c) or be heavily biased towards that region (Brooksby *et al* 2003, Li *et al* 2003). The degradation in image quality due to uncertainties in the anatomical prior, and the best way to minimize this degradation, are as yet uncertain (Schweiger and Arridge 1999b). Including prior anatomical information has advantages for both linear and non-linear reconstruction (Boas *et al* 2004a).

Another approach is to express (8) as a statistical inverse problem in a Bayesian framework. Bayes' theorem can be written as $p(x|y) \propto p(y|x)p(x)$ where $p(x|y)$ is the posterior probability of obtaining the image x given the data y , $p(y|x)$ is the likelihood of obtaining y given x (which is obtained by solving the forward problem), and $p(x)$ is the prior density, which in these terms is simply an estimate, made before carrying out the experiment, of the most likely image. If we assume that the distribution of errors is Gaussian, then Bayes' theorem takes the form

$$p(x|y) \propto \exp(-\|y - f(x)\|^2) \exp(-\|\Pi\|^2) \quad (10)$$

where the likelihood $p(y|x) \propto \exp(-\|y - f(x)\|^2)$ and the prior $p(x) \propto \exp(-\|\Pi\|^2)$. The value of x which maximizes (10) is the *maximum a posteriori* (MAP) estimate. Maximizing (10) is equivalent to minimizing its negative logarithm, which is (8), but can offer further approaches which deal with prior information and covariance estimates in a direct and intuitive manner (Kwee 1999, Kohlemainen 2001, Mosegaard and Sambridge 2002, Evans and Stark 2002, Oh *et al* 2002).

Recently, efforts have been made to incorporate Monte Carlo techniques into the inverse problem. Standard Monte Carlo techniques are too slow to be used for practical image reconstruction, although faster methods are available. One example is the Metropolis–Hastings algorithm which is an example of a Markov chain Monte Carlo (MCMC) technique, in which individual photon steps are drawn from a biased random walk which is chosen to minimize the number of discarded photons (Mosegaard and Sambridge 2002). These techniques have been used as the basis of image reconstruction algorithms in EIT (Kaipio *et al* 2000, West *et al* 2004), partly because the Monte Carlo simulations form a probability density which can be interpreted as the Bayesian maximum *a posteriori* estimate, leading very naturally to a statistical expression of the inverse problem (Evans and Stark 2002).

The approaches discussed above assume that the prior information, whether in terms of the data covariance or the image statistics, is governed by Gaussian statistics. This is not necessarily the case: a Poisson model for the data may be more appropriate if photon counting errors are significant, and assuming that the pixel values are distributed as Gaussian random variables forces the image to be homogeneously and isotropically smooth. The latter issue has been identified as a significant weakness and has been addressed in two ways. First, Kaipio *et al* (1999) introduced an inhomogeneous, anisotropic image covariance term which allowed, for example, a change in optical properties in the brain to be correlated more closely with neighbouring pixels in the brain than with those in the skull. A second approach is to minimize the total variation, defined as the integral of the absolute gradient of the image, rather than the L2-norm (Borsic 2002). The L2-norm forces the image to be smooth, and is optimal if the optical properties are distributed as a Gaussian random field. If the distribution of optical properties is known to be piecewise constant, the L2-norm will smooth the image, whereas minimizing total variation will reduce oscillations in the image but still allow boundaries to be sharp. Other non-Gaussian priors may be considered.

3.4.5. Methods that exploit symmetry. Some improvements to speed and robustness of the inverse problem can be obtained for systems that possess symmetry. Examples are rotational symmetry in a cylinder or sphere, or translational symmetry in a slab. It is easiest to develop this idea for the analytical version of the linear inversion kernels based on Green’s functions. Green’s functions are the kernels of the inverse solver for a PDE, and when the domain possesses symmetry, the PDE may often be solved by a separation of variables technique, which implies that the inversion kernels can be expressed as the product of functions in the separated variables. In the work of Markel and Schotland (2001), the slab geometry gives rise to a product of transverse plane waves and one-dimensional integral equations in the perpendicular direction. It is this decoupling of transverse propagating waves and perpendicular scalar waves that allows faster inversion of a set of one-dimensional integral equations, rather than one coupled 3D integral equation. The solution of these linear equations builds up a solution in the basis of the transverse component, which can then be transformed into image space by a fast transform method. Similar methods apply in the cylindrical and spherical geometries where the transverse components are Fourier and spherical harmonic waves respectively. Furthermore the case where only part of the data is sampled can be included by convolution with a masking function. Finally Markel *et al* (2003) considered extension to the non-linear case by applying an iterative method, linearized around the symmetric case.

As well as the analytical case, a discrete implementation such as FEM can also be developed. This approach was developed by Metherall *et al* (1996) for EIT, and applied to optical tomography by Hampel and Freyer (1998).

3.4.6. Solving for coupling coefficients. The measured data in optical tomography depend not only on the properties of the object under examination, but also on the characteristics of the source and detector fibres, instabilities in the source power and detector efficiency, and on the efficiency with which light is coupled into and out of the medium. A well-designed calibration procedure can minimize the effects of the optical fibres and the instrumentation (Hillman *et al* 2000, McBride *et al* 2001) but characterizing the coupling between the fibres and the tissue can be more difficult. One approach which has been successfully adopted, particularly with regard to optical topography, is difference imaging, in which images are reconstructed using the difference between measurements recorded at two states in such a way that coupling effects cancel (section 4.1). Alternatively, images can be reconstructed using temporal data only (Hebden *et al* 2002), although this may reduce the ability to separate the absorption and scattering properties. These approaches are not always appropriate, however, and so techniques have been developed to correct for coupling effects during image reconstruction.

Schmitz *et al* (2000) and Boas *et al* (2001b) introduced a method for solving for the unknown coupling coefficients as part of the image reconstruction problem. Each source and detector was associated with a complex coupling term. A measurement M_{ij} between source i and detector j was modelled as $M_{ij} = S_i D_j m_{ij}$ where S_i and D_j are the source and detector scaling factors and m_{ij} is the ‘ideal’ measurement, depending only on the internal optical properties of the object. The reconstruction problem is then posed in terms of minimizing the difference between the measured data and $S_i D_j m_{ij}$, where S_i and D_j are solved for in the inverse problem. Images could be reconstructed successfully if up to 80% uncertainty in amplitude was added to simulated data (Boas *et al* 2001b). The technique has since been extended to allow small errors in optode position to be corrected (Stott *et al* 2003, Culver *et al* 2003c) and has been used for dynamic breast imaging (Intes *et al* 2003). Vilhunen *et al* (2004) have implemented a related method which can be used when the sources and detectors have rotational symmetry. Oh *et al* (2002) used a Bayesian formulation to reconstruct 3D images non-linearly by treating the unknown source–detector coupling coefficients as unwanted ‘nuisance’ parameters.

3.4.7. Use of dynamic information. Image reconstruction is generally applied to the spatial domain but additional information can be obtained by examining the temporal evolution of the signal. Physiological signals from the heart rate, ventilation and blood vessels are time dependent. If the image acquisition time is short compared to the physiological fluctuations, an image time series can be obtained, which can then be processed to give dynamic images showing parameters such as the covariance or the amplitude and phase at a particular frequency of physiological interest (Barbour *et al* 2001, Graber *et al* 2002).

A different situation occurs when the image acquisition rate is not short compared to the physiological changes. In this case, the optical properties change during the acquisition of each image and so a straightforward static image reconstruction would not be valid. The Kalman filter technique has been used to model the image space as a state whose properties evolve with time in a known manner, the details of which are supplied as prior information. It may be expressed as

$$x_{t+1} = \mathbf{K}x_t + n_t, \quad (11)$$

where x_t is the image x at time t , \mathbf{K} is the state transition matrix and n_t is additive noise at time t . In the simplest case, \mathbf{K} is the identity matrix, in which case the update is a random walk. This approach helps to condition the inverse problem by using the current state, and knowledge of how it evolves, to constrain the possible solutions for the next state. It can be used to image events which occur on a shorter time scale than the image acquisition by calculating an updated

image using the Kalman filter when only a limited subset of data has been acquired. This is ideally suited for systems which acquire data from sources sequentially but the detectors simultaneously, in which case an updated state can be estimated when each source is activated. This approach has been successfully applied to both simulated data (Kohlemainen *et al* 2003) and real data (Prince *et al* 2003) in optical tomography. Eppstein *et al* (2001, 2002) have developed an image reconstruction technique for fluorescence tomography which uses the Kalman filter to update each iteration of a static non-linear reconstruction procedure.

3.4.8. Recovery of object shape. Another approach to optimizing the use of data in optical tomography is not to reconstruct for a large number of image pixels, which leads to a highly underdetermined problem, but instead to reconstruct for the boundaries and properties of internal regions which can be assumed to have piecewise constant optical properties.

One method to solve for the boundaries of internal regions is to formulate a minimization problem where the image parameters are the Fourier coefficients of the smooth region boundaries. This was first solved assuming the optical properties of the regions are known *a priori* (Kohlemainen *et al* 1999), and later extended to solve simultaneously for both the region boundaries and the optical properties (Kohlemainen *et al* 2000a). A further refinement was to use an initial static image reconstruction to identify the number of regions and their approximate locations before finally solving for the boundaries and optical properties of the regions (Kohlemainen *et al* 2000b). In 3D, it may be more appropriate to assume that regions of interest are ellipsoidal and to solve for the parameters of the ellipse rather than Fourier components (Kilmer *et al* 2003).

A promising technique for the inverse shape estimation problem is provided by representing internal regions using a level set function. This is a function which is 1 inside the regions and 0 elsewhere. This method assumes that the optical properties of the background and regions of interest are known, but does not place constraints on the number of regions or their shapes. Dorn (2002) implemented this method, thresholding an initial spatial reconstruction to provide a starting estimate for the internal objects which are then described using a level set whose boundaries evolve as the reconstruction progresses.

4. Clinical applications

4.1. Imaging brain function with optical topography

For more than two decades, the single channel measurement technique of NIR spectroscopy (NIRS) has been successfully used to measure the haemodynamic response to brain activity in both adults and neonates (Hoshi 2003, Ferrari 2004). It has been used to record functional activity for research into brain cognition, and to examine brain development in infants (Obrig and Villringer 2003). An obvious limitation of NIRS is the lack of any spatial information. It is natural to consider combining multiple NIRS measurements in order to localize the origin of signals in the brain; indeed, the first optical topography studies were carried out in this way (Gratton *et al* 1995).

NIRS and optical topography measure the haemodynamic response following brain activation and therefore rely on the spatial and temporal variability in the concentration and oxygenation of haemoglobin in the blood. The penetration depth of optical topographic systems is generally assumed to be approximately half the optode spacing. For typical spacings around 25–35 mm, this gives a penetration depth of about 15 mm, which is sufficient for sampling the adult cortex. Recent reviews of optical topography have been provided by Strangman *et al* (2002a), Hebden (2003) and Koizumi *et al* (2003).

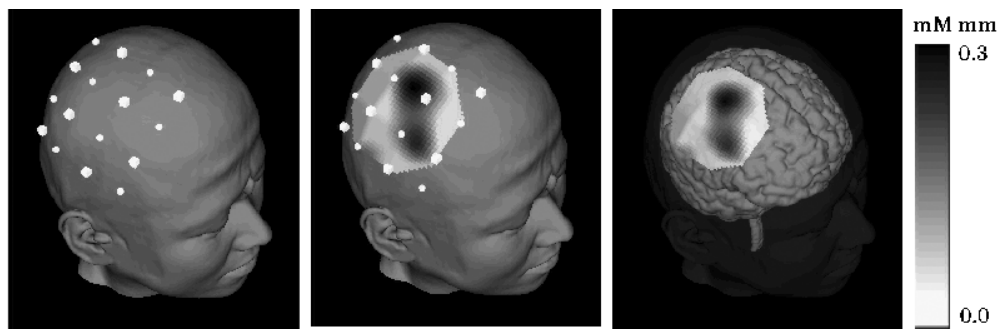


Figure 3. An optical topography image obtained using the Hitachi ETG-100 system showing [HbO] during a motor task mapped onto the MR image of a normal volunteer. Activation is seen in the right motor cortex following gripping of the left hand (reprinted from Kawasaki *et al* (2002), with permission from Elsevier).

The most commonly used method for imaging brain function is functional MRI, which is sensitive to the blood oxygen level dependent (BOLD) signal. BOLD MRI detects signal changes caused by the magnetic susceptibility of HHb being greater than that of HbO and other brain tissues, and generates images of these changes in a few seconds. It is currently viewed as the ‘gold standard’ for functional brain imaging due partly to the ability to register fMRI images directly onto a structural MR image taken during the same examination. However, optical topography does have some advantages over fMRI which have led to it developing an increasing role in functional brain imaging. For example, images can be acquired very rapidly (a 50 Hz acquisition rate has been demonstrated by Franceschini *et al* (2003)), and it is inexpensive and portable, enabling images to be obtained at the bedside or in the laboratory. Moreover, mechanisms which generate the NIRS signal are closely correlated with the BOLD signal of fMRI but add information by distinguishing quantitatively between changes in [HHb] and [HbO] (Strangman *et al* 2002b). The primary drawback of optical imaging is the inherently low spatial resolution, which is about 10 mm at best. However, although the spatial resolution of fMRI is typically 3 mm and can be as good as 1 mm, the image processing techniques which are commonly used model the image as a smoothed random field and so impose a smoothing filter with a 8–10 mm Gaussian kernel before analysis (Turner and Jones 2003). In certain circumstances, therefore, there may be little difference between the effective spatial resolutions of the two techniques.

Optical topography of the adult brain has been largely pioneered by researchers from the Hitachi Medical Corporation (Tokyo, Japan), who have used the ETG-100 Optical Topography System (figure 3), described in section 2.2, to examine a range of cognitive tasks (Takahashi *et al* 2000, Koizumi *et al* 2003). Optical methods are well suited for imaging tasks related to language, as the investigation is silent, unlike fMRI (Watanabe *et al* 1998). Optical topography is beginning to be routinely applied to pathological conditions: Watanabe *et al* (1998, 2002) showed that optical topography could detect changes in [HbO] and [HHb] during epileptic seizures, and Matsuo *et al* (2003) showed a difference in the response to viewing traumatic images between normal controls and patients who suffered post traumatic stress disorder from the 1995 sarin nerve gas attack on the Tokyo subway. Meanwhile, Obata *et al* (2003) showed that visual evoked responses were not affected by alcohol.

Franceschini *et al* (2003) have used a related approach to image the sensorimotor cortex using a system with eight laser diode sources at each of two wavelengths and 16 detectors. Each channel was frequency-encoded, allowing all the sources and detectors to be active simultaneously and decoded in software to maximize the image acquisition rate. Using this

method, images could be obtained at 50 Hz. They found an increase in [HbO] and a decrease in [HHb] contralateral to the stimulated side with a reduced ipsilateral response, consistent with equivalent fMRI and PET studies.

The Hitachi approach generates images by assuming that a change in intensity originates midway between the source and detector which measured that change. The image is produced by mapping the changes according to the positions of the appropriate source–detector pair. This technique has some drawbacks: the spatial resolution cannot be better than the optode spacing, it is difficult to apply it to irregular arrangements of connectors, and it does not naturally allow the inclusion of prior information (Yamamoto *et al* 2002). These limitations have been addressed by Boas *et al* (2001c) who showed that a linear reconstruction approach improves the quantitative accuracy compared to single channel NIRS measurements (and, by implication, images generated by mapping, which are equivalent to multiple NIRS measurements). Furthermore, such an approach allows multiple topographic measurements to contribute to each pixel, which can yield a twofold improvement in spatial resolution and localization accuracy (Boas *et al* 2004a, 2004b). Culver *et al* (2003c) have used a similar approach based on linear reconstruction to image the rat cortex.

Most optical topographic images have been obtained using systems which measure intensity alone, meaning that the effects of μ_a and μ'_s cannot be uniquely separated (Arridge and Lionheart 1998). This has been addressed by Franceschini *et al* (2000) who used a frequency-domain system to acquire images of activity in the adult cortex with a time resolution of 160 ms. The system uses eight sources at each of two wavelengths (758 and 830 nm) and two detectors, and is produced commercially by ISS Inc., USA. Toronov *et al* (2001a) used a similar system to record optical data during motor activity simultaneously with fMRI images. They found close spatial and temporal agreement between the optical and BOLD signals. In a related study, Toronov *et al* (2001b) showed that both the amplitude and the phase of the NIRS signal correlated with the BOLD response.

Optical imaging techniques are particularly well suited to imaging infants, being portable and somewhat less sensitive to motion artefact than fMRI. The first report of optical topography on premature babies was by Chance *et al* (1998a) who used a system with nine sources and four detectors on adults and on a four-week-old neonate. The system measured intensity only but used a phase cancellation technique to improve sensitivity. Sources were arranged on a grid and a signal applied to alternate sources at phase shifts of either 0° or 180° such that, in a homogeneous medium, the phase shift is 90° and the amplitude is zero directly between the sources, where the detectors are placed. The Hitachi systems have also been used to investigate brain activity in infants. Taga *et al* (2000) observed spontaneous fluctuations in [HHb] and [HbO] in eight sleeping neonates with periods of 8–11 s which were attributed to vasomotion. Oscillations in [HHb] led those in [HbO] by $3\pi/4$, which was explained by a localized increase in brain activity leading to an increase in [HHb], followed by an increase in cerebral blood flow which supplies additional oxygen to increase [HbO]. A similar effect has been observed in BOLD fMRI. More recently, the same group examined 20 infants a few months old and were able to record images during visual activation from eight infants (Taga *et al* 2003). The other 12 were rejected due to movement, crying, lack of attention and poor contact due to hair. They concluded that the convenience of optical topography represented a significant advantage over other techniques. Kusaka *et al* (2004) carried out a similar study using a CW system supplied by Shimadzu Corporation and showed different responses between adults and infants. Higher cognitive functions have also been imaged using the Hitachi system—Peña *et al* (2003) showed that the temporal cortex in neonates is activated more strongly by normal speech than by speech played backwards, and Tsujimoto *et al* (2004) showed that the same area of the brain, the lateral prefrontal cortex, appears to be responsible

for working memory in both adults and pre-school children. Both of the latter two articles comment on the convenience with which optical topography can be used to image babies and children. Vaithianathan *et al* (2004) have built and tested a CW topography system with an interface consisting of a flexible pad, designed to be conveniently applied to an infant's head.

Hintz *et al* (2001) used a CW topography system to image passive motor activity in premature infants. Their system acquires a total of 144 independent measurements in approximately 3 s, and images were reconstructed using a non-linear approach. Bluestone *et al* (2001) used an even more sophisticated image reconstruction technique to generate 3D images of a region of interest beneath the adult forehead during a Valsalva manoeuvre, in which the intrathoracic pressure is increased (and therefore cardiac output decreased) by expiration against a closed airway. They used a CW system (Schmitz *et al* 2002) to acquire data from 15 optodes on the forehead with a temporal resolution of 3 Hz.

Optical topography has been extensively used to image functional brain activity in both adults and neonates. During the past five years it has evolved beyond a laboratory technique to be used to address hypothesis-led questions about neurophysiology and brain development. It has unique advantages over other brain imaging techniques, including its excellent temporal resolution and its ability to distinguish between [HHb] and [HbO]. It can be used in a natural, relaxed environment, making it well suited for psychological studies, and it can be used to image awake infants.

4.2. Imaging the neonatal brain with optical tomography

Optical topography is able to measure and display haemodynamic changes occurring in the cortex, but is far less sensitive to deeper tissues. Optical tomography, however, uses widely spaced sources and detectors to measure light which has passed through central regions of the brain, which can be affected by disruption to the supply of blood and oxygen around birth. Light travelling through these regions is heavily attenuated and therefore more intense light sources and more sensitive detectors are required. Even so, the acquisition time is typically a few minutes compared to less than a second in the case of optical topography.

Brain injury in pre-term and term infants is a major cause of permanent disability and death. Several groups have developed optical tomography of the infant brain with the aim of providing diagnostic and therapeutic information about the more important types of brain injury. Intraventricular haemorrhage (IVH) may occur in premature infants whose cerebral vasculature is too weak to withstand the fluctuations in blood pressure which occur during birth (Whitelaw 2001), while periventricular leucomalacia is damage to the white matter which is common in premature infants (Volpe 2001). Hypoxic-ischaemic brain injury around the time of birth is a major cause of brain injury in the term infant (Wyatt 2002). These three mechanisms of brain injury all manifest themselves as disruption to the supply of blood and oxygen to vulnerable areas of the brain. Currently, they are either diagnosed clinically, by ultrasound (which gives only anatomical information) or MRI (which clinicians may be reluctant to request if it means moving a very ill infant out of an intensive care environment). Optical tomography may provide a bedside system to identify infants at risk, to diagnose injury and to monitor treatment (Thoresen 2000). For a detailed review of optical imaging of the neonatal brain, see Hebden (2003).

The first tomographic images of the neonatal were recorded by the group of Benaron, by reconstructing measurements of mean photon flight time made across the neonatal head. Thirty-four pairs of sources and detectors were attached to the head using a headband (Hintz *et al* 1998) and were used to obtain 2D tomographic slice images of anatomical disorders (Hintz *et al* 1999, Benaron *et al* 2000) and functional activation (Benaron *et al* 2000). Eight

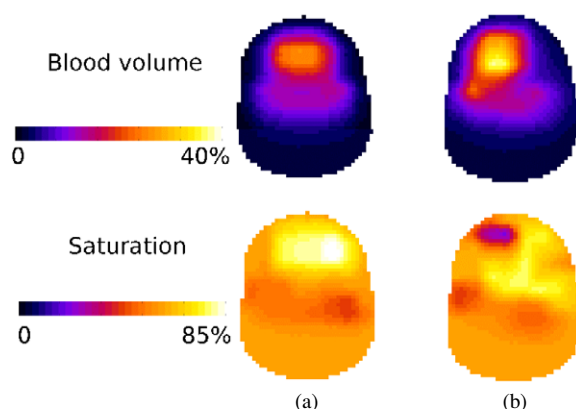


Figure 4. Optical tomography of the neonatal brain. The central column shows coronal slices through 3D images of blood volume and oxygen saturation in an anatomically normal four-week-old baby, born at 28 weeks. The column on the right shows equivalent images, reconstructed from the first baby's identical twin who had a left ventricular haemorrhage. The haemorrhage can be seen as an increase in blood volume and a decrease in oxygen saturation.

optical images were generated from six infants in the first month of life, four of whom had IVH. Six of the eight images compared favourably with CT, ultrasound and MRI images. Later, Benaron *et al* (2000) generated images from two neonatal subjects, one a control and the other with a stroke. They detected a significant difference between the two subjects, and the location of the stroke agreed with a CT image. Images were also presented, using the same approach, of functional motor activity. The images obtained in these studies were remarkable, given the relatively simple instrumentation (Benaron *et al* 1994b) and crude reconstruction techniques (Benaron *et al* 1994a), and encouraged the suggestion that optical tomography could play a major diagnostic role in neonatology.

More recently, the group at University College London has used a purpose-built 32-channel time-resolved imaging system (Schmidt *et al* 2000) and a non-linear image reconstruction approach based on finite element modelling (Arridge *et al* 2000b) to generate 3D images of the neonatal head. Sources and detectors are coupled to the head using a foam-lined helmet which is custom built for each infant. The positions of the connectors within the helmet are used to define the outer surface of a finite element mesh (Gibson *et al* 2003) which is used for image reconstruction. The first published results were images of the brain of an infant with IVH, which revealed an increase in blood volume in the region of the haemorrhage as shown on an ultrasound examination (Hebden *et al* 2002). Another of the babies studied so far was mechanically ventilated, allowing images to be reconstructed from data acquired at two wavelengths during changes in inspired oxygen and carbon dioxide (Hebden *et al* 2004b). The reconstructed images of [HHb] and [HbO] agreed qualitatively with physiological predictions. Recently, images have been obtained from a pair of twins, recorded consecutively on the same day. One twin was anatomically normal while the other had an IVH which had caused additional bleeding into the brain tissue. Images of blood volume and oxygenation in the baby with the normal brain (figure 4(a)) are symmetrical about the midline and appear to show a decrease in blood volume in the white matter. The haemorrhage (figure 4(b)) can be seen as an increase in blood volume and a decrease in oxygenation (from about 65% to about 10%). The location of the increase in blood volume correlated well with the site of the IVH determined from an ultrasound image, but interestingly, the location of the increase in

oxygenation appeared to correlate more closely with the infarct of the haemorrhage into the brain tissue.

Encouraging results have been obtained by neonatal optical tomography, although so far the application is not as widely used as optical topography. This is partly due to the additional complexity of the instrumentation and the practical difficulties of acquiring data from premature babies who may be very ill. A further difficulty is obtaining an adequate reference measurement for data calibration. Theoretical advances such as solving for the coupling coefficients and the incorporation of prior anatomical information from MRI and improvements to instrumentation are expected to lead to significant improvements in image quality and clinical acceptance.

4.3. Optical mammography

In 2000, more than 1 million women were diagnosed with breast cancer worldwide (Ferlay *et al* 2001). Early detection decreases mortality (Tabar *et al* 2003), so many countries routinely screen for breast cancer. X-ray mammography is the screening method of choice (Fletcher and Elmore 2003) but its effectiveness may depend on issues such as the age of the woman, family history of cancer, body mass index, the use of hormone replacement therapy, the use of computer-aided detection, and the availability of additional clinical or imaging information (Blarney *et al* 2000, Warren 2001, Houssami *et al* 2004, Banks *et al* 2004). It requires ionizing radiation and its benefits for younger women are unclear (Lucassen *et al* 2004). Other imaging modalities such as MRI and ultrasound may be useful in certain circumstances but neither is suitable for screening of asymptomatic women (Morris *et al* 2003, Warner *et al* 2004).

It is well known that tumours are associated with increased vascularization (Rice and Quinn 2002) so optical methods provide a natural method for both interrogating tissue to identify disease and for spectroscopically determining the blood volume and oxygenation of a suspicious lesion seen on x-ray mammography to improve specificity. A major disadvantage of optical mammography is the inherently poor spatial resolution. A successful screening tool must be able to identify tumours smaller than 1 cm, as mortality increases rapidly for tumours which exceed this size (Webb *et al* 2004). Because of this, optimizing spatial resolution is an important concern in optical mammography. Researchers are also exploring other uses of optical mammography which are less dependent on resolution, such as staging previously identified suspicious lesions, and monitoring the response to new and existing forms of therapy. One of the attractions of the technique is its suitability for repeated investigations on the same subject.

Despite many previous efforts to determine them, the *in vivo* optical properties of healthy breast tissues and common lesions are not fully known. Most early work (e.g. Peters *et al* (1990)) concentrated on measuring the properties of breast tissue *in vitro* and, as blood and water are the primary chromophores, it is not clear how *in vitro* values relate to the intact breast. Even optical properties measured *in vivo* will depend on the geometry of the measurement (particularly if the breast is compressed) and the model used to derive the optical properties from the measurements. Measurement at a single location can give information only about the local average properties. Even so, such measurements have been shown to correlate with age, body mass index and menstrual state (Shah *et al* 2001, Cerussi *et al* 2001). Perhaps the most reliable measurements of breast optical properties to date are those of Durduran *et al* (2002), who obtained frequency-domain measurements at 750, 786 and 830 nm in 52 women using a parallel plate geometry with gentle compression. The average optical properties (\pm standard deviation) were $\mu_a = 0.0041 \pm 0.0025 \text{ mm}^{-1}$, $\mu'_s = 0.85 \pm 0.21 \text{ mm}^{-1}$ (at 780 nm),

blood volume = $34 \pm 9 \mu\text{M}$ and oxygen saturation = $68 \pm 8\%$. These values agree with other published *in vivo* values (e.g. Suzuki *et al* (1996)), but the μ_a is approximately double that of corresponding *in vitro* measurements, possibly because of the lower blood volume in excised breast tissue. Grosenick *et al* (2004b) measured the optical properties of tissue and tumour in 50 women at 680 and 785 nm by assuming a spherical tumour in an infinite, homogeneous slab. They found that μ_a in the tumour was between two and four times that of surrounding tissue due to the increased blood volume, and μ'_s was slightly elevated. These results agree with similar measurements made by Fantini *et al* (1998) and Chernomordik *et al* (2002b). Holboke *et al* (2000) report a similar increase in μ_a but a 50% reduction in μ'_s .

A number of alternative approaches to optical mammography have been evaluated. Most clinical studies have been performed using instruments which compress the breast, though generally more gently than in x-ray mammography. This reduces the attenuation of the transmitted light and ensures that the geometry of the problem is well known. The breast is compressed between either two parallel arrays of sources and detectors, or between plates over which individual sources and detectors are scanned in a rectilinear manner. However, the latter method is only suitable for generating projection images (analogous to x-ray mammograms) since it does not yield sufficient depth information for a 3D reconstruction.

Groups based in Berlin and Milan have between them performed more than 300 clinical studies as part of Optimamm, a consortium funded by the European Union (see www.optimamm.de and a forthcoming special issue of *Physics in Medicine and Biology*). Both systems acquire time-domain measurements at multiple wavelengths by scanning a single source and detector in tandem across a gently compressed breast. The Milan group have explored the effect of using a wide range of wavelengths (Pifferi *et al* 2003, Taroni *et al* 2004a), and the Berlin group have investigated the benefits of acquiring additional 'off-axis' measurements (Grosenick *et al* 1999). Figure 5 shows an optical mammogram recorded by Grosenick *et al* (2003) with two views of a tumour in the left breast of a patient, and the corresponding images of the healthy right breast. Both groups report that they can successfully identify around 80–85% of radiologically identified tumours (Grosenick *et al* 2004a, Taroni *et al* 2004b), and it is likely that second generation systems which incorporate improved spatial and spectral discrimination will yield improved detection rates.

Compressed breast geometries have also been evaluated for imaging by Pera *et al* (2003) using a frequency-domain instrument built by Siemens Medical Engineering, and by Culver *et al* (2003a) using a hybrid system which determines the bulk optical properties using frequency-domain measurements and spatial information from up to 10^5 continuous wave measurements (see section 2.4).

One of the potential disadvantages of breast compression is the corresponding reduction in the blood volume. Although this improves overall transmission, blood represents the principal source of contrast between tissues, and the most likely means by which tumours may be identified and characterized. Several groups avoid compression by surrounding the breast with rings of sources and detectors. This arrangement is also ideal for generating 3D images. The main disadvantage of this approach is that a much greater volume of tissue is sampled, and therefore the detected light intensities are much lower and have a greater dynamic range than for the compressed breast geometry.

The 3D breast imaging approach has been pioneered by the group at Dartmouth College. They are exploring optical mammography as part of a larger study involving four different breast imaging modalities (optical, impedance, microwave and MR elastography (Poplack *et al* 2004)). They use a frequency-domain optical tomography system (McBride *et al* 2001) with six laser diodes operating at wavelengths from 660–836 nm multiplexed to 16 source positions, and 16 detectors, located around the circumference of a 2D ring whose diameter

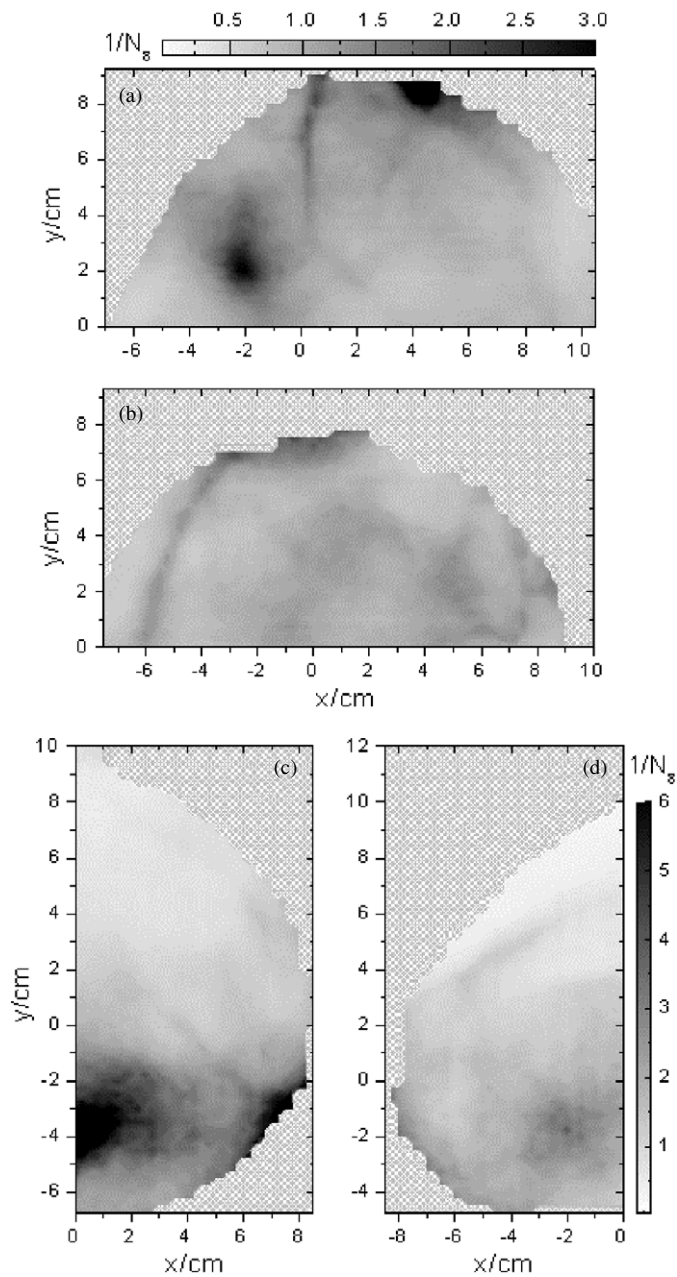


Figure 5. Optical mammogram obtained by Grosenick *et al* (2003). (a) Left breast, craniocaudal, with tumour at $(x, y) = (-2 \text{ cm}, 2.5 \text{ cm})$; (b) right breast, craniocaudal; (c) left breast, mediolateral, with tumour centred at $(x, y) = (0.5 \text{ cm}, -3.75 \text{ cm})$; (d) right breast, mediolateral.

can be varied to fit the breast. 3D images are reconstructed from three 2D data sets, each consisting of amplitude and phase measurements (Dehghani *et al* 2003b). Recently, the group has successfully extended their technique to reconstruct directly for haemoglobin and water concentrations, blood oxygenation and scattering parameters (Pogue *et al* 2004). A similar approach has been investigated by Jiang *et al* (2002) using a single-wavelength CW system.

The 32-channel time-resolved system at UCL has also been used to generate 3D images of the uncompressed breast, either by using a 2D ring of connectors or a 3D hemispherical tank filled with a tissue matching fluid (Yates *et al* 2004), an approach originally employed for the prototype developed by Phillips Medical Systems (Colak *et al* 1999).

A sophisticated CW system for imaging both breasts simultaneously has recently been presented by Barbour *et al* (2004). It is designed to acquire images which reveal haemodynamic phenomena within the breast.

Because the prognosis for breast cancer depends largely on the size of the tumour, the relatively poor spatial resolution of optical mammography may limit its use in routine screening. However, the technique may provide a powerful method for the examination of suspicious lesions previously identified by other means. With this in mind, attempts have been made to use the prior information from other medical imaging techniques to condition the optical image reconstruction. In principle, this will allow images with the excellent physiological information content of optical imaging to be reconstructed with the high spatial resolution provided by MRI, ultrasound or x-ray mammography. Ntziachristos *et al* (1998) built and tested a combined MR/optical imaging system and successfully used it to record optical and MR images from volunteers with a range of benign and malignant lesions (Ntziachristos *et al* 2000, 2002c). Li *et al* (2003) built an optical imaging probe which was interchangeable with a standard film cassette in an x-ray mammography tomosynthesis instrument. They used this combined system to generate 3D x-ray images of the compressed breast which they segmented into 'suspicious' and 'background' regions, which were then used as anatomical prior information in the optical tomography image reconstruction. The spatial resolution of the optical image was enhanced such that the reconstructed absorber was confined to a volume even smaller than the suspicious region identified in the x-ray images (see figure 6).

Exogenous contrast media can also be used to improve the sensitivity to small lesions. The most widely used contrast agent is indocyanine green (ICG), which has been approved for use on human subjects by the US Food and Drug Administration as an NIR absorbing and fluorescing dye, and has been used for breast imaging by Ntziachristos *et al* (2000) and Intes *et al* (2003). When injected intravenously, ICG binds immediately and totally to blood proteins, primarily albumin. This ensures that ICG is confined almost entirely to the vascular compartment except for incidences of abnormal blood capillaries with high permeability, as in the case of tumours with high vascularity. Thus ICG is primarily an indicator of blood volume, although it provides a certain degree of specificity for some types of tumour. Other, more selective contrast agents and fluorescent dyes for breast cancer detection are currently being evaluated in animal models (Ntziachristos and Chance 2001) (see section 4.5 below).

One of the attractive benefits of using contrast agents for optical tomography is that the imaging process involves reconstructing a *change* in optical properties, which is generally more tolerant of experimental and modelling errors. Therefore the use of contrast agents could lead to significant improvements in image quality, albeit at the expense of a more invasive investigation.

4.4. Other tissues

The application of optical imaging to other areas of the body is restricted by the limited penetration of light across large thicknesses of tissue. Muscle tissue has been widely investigated using NIRS, although relatively few optical imaging studies have been reported. The forearm muscle has probably been the most frequently studied, the first time by Maris *et al* (1994) using a frequency-domain optical topography system to map differences in the

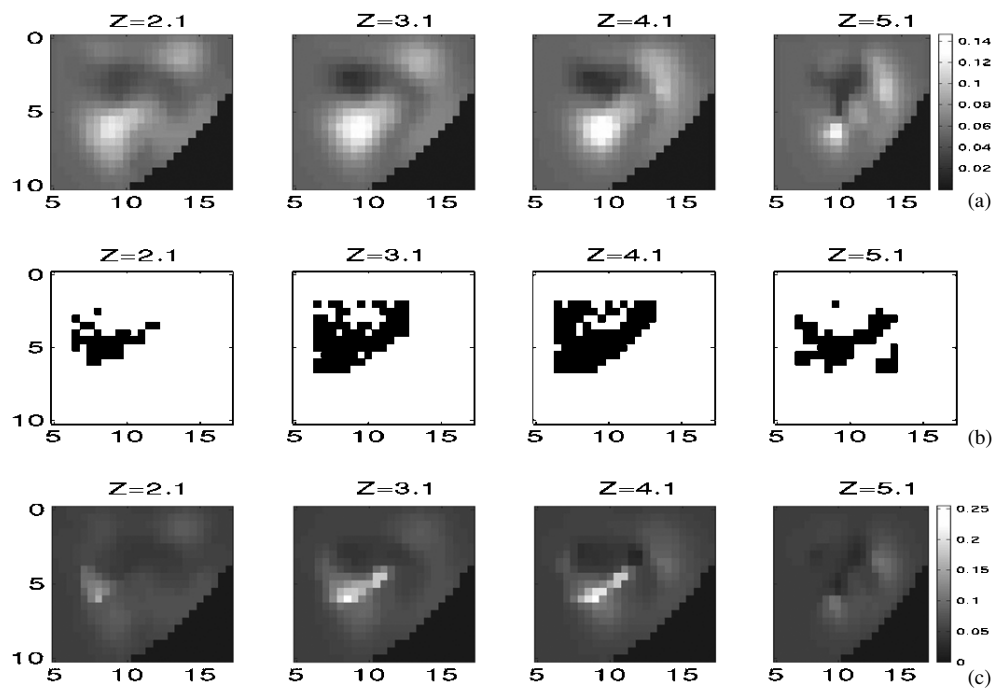


Figure 6. Optical mammography using spatial prior information from x-ray mammography (Li *et al* 2003). (a) Absorption image reconstructed from clinical optical mammography data using conventional linear Tikhonov reconstruction; (b) corresponding x-ray mammography image, thresholded to highlight regions suspected of having a lesion; (c) optical mammography image reconstructed from clinical data using (b) as spatial prior.

haemoglobin oxygenation in finger extensor muscles during exercise. Graber *et al* (2000) have used a CW optical tomography system for a series of real-time dynamic arm imaging experiments, and Araraki *et al* (2000) and Hillman *et al* (2001) have used time-domain systems to measure changes in tissue absorption in response to finger flexion exercises at two wavelengths from which cross-sectional images of haemoglobin concentration were reconstructed.

Another relatively advanced application of diffuse optical imaging is the examination of the finger for rheumatoid arthritis. Hielscher *et al* (2004) have produced images by scanning a single source and detector along the finger, in which contrast is provided by an increase in blood volume due to inflammation and changes in the optical properties of the synovial fluid. Because the synovial fluid is low scattering and the diameter of the finger is small, the diffusion approximation may not be appropriate for image reconstruction (Hielscher *et al* 1999). Similar work is being carried out by Xu *et al* (2001, 2002b) who have generated 3D images using the diffusion approximation from continuous wave data.

A related application, which could prove to be clinically significant but is not yet an imaging technique, is the optical examination of the heel bone, which is routinely examined by x-ray in middle-aged women to detect osteoporosis. Pifferi *et al* (2004) have obtained preliminary transmission spectra through the heel and found that the bone mineral density (determined from the absorption spectrum of bone) decreased with age in seven volunteers. Ugryumova *et al* (2004) have proposed a similar application based on optical coherence tomography.

4.5. Molecular imaging

Molecular imaging is a rapidly growing research field in which contrast agents are bound to specific proteins or genes and used to image the distribution of targeted molecules in small animal models (Weisslader and Ntziachristos 2003, Cherry 2004). The recent growth in molecular imaging has largely been triggered by the success of the Human Genome Project and improvements in biochemical techniques. Molecular imaging has traditionally involved tracking radioactive tracers (Goertzen *et al* 2002, Comtat *et al* 2002) but optical techniques, particularly fluorescence imaging, are increasingly finding a role (Cubeddu *et al* 2002, Ntziachristos *et al* 2002b). Combining the new contrast agents with diffuse optical imaging in animal models is likely to become a very powerful tool in the development of new drugs and the study of haemodynamics in animal models (Culver *et al* 2003b).

Several interesting theoretical issues must be addressed in molecular imaging. The animal typically used in drug development is small compared to human organs and photons may travel only a few transport scattering lengths before detection. This means that the diffusion approximation may not be valid, and therefore higher order approximations are required (Klose and Hielscher 2003). Because of the difficulty of attaching optical fibres to such a small experimental model, Schulz *et al* (2003, 2004) have developed non-contact imaging techniques, based on first determining the surface of the animal and then solving a forward model where a free-space region is coupled to a diffusive region. Hillman *et al* (2004) have developed an approach, designed for imaging the rat cortex, in which a microscope acts as a non-contact source and detector, providing data which are modelled using a Monte Carlo simulation and reconstructed using diffuse optical tomography techniques. The use of prior information in optical molecular imaging is also valuable, both to assist the optical image reconstruction (Xu *et al* 2003) and to independently validate the optical results (Siegel *et al* 2003).

Fluorescence imaging is ideally suited to molecular imaging as the small penetration depths in small animals ensure that a strong signal is obtained. However, Ntziachristos *et al* (2002a) are optimistic that, given improvements in detector technology, it will be possible to measure a fluorescence signal across the breast, and Godovarty *et al* (2004) have already measured fluorescence signals across a breast-like phantom. Progress in this area could lead to development of a range of valuable clinical techniques (Ntziachristos and Chance 2001). Fluorescence imaging of the breast has been reviewed in detail by Hawrysz and Sevick-Muraca (2000).

5. Future challenges

5.1. Experimental techniques

Improvements in source technology are likely to dominate developments in instrumentation. The development of new laser diodes has had a major impact on systems designed for diffuse optical imaging, and further improvements in the technology are anticipated. Higher power will allow increased penetration and faster image acquisition. Significant improvements can be expected from a combination of better theoretical understanding of the optimal combinations of wavelengths for a particular application, and the availability of sources at a wider range of wavelengths.

Molecular imaging is a developing application for diffuse optical imaging techniques, driven partly by the rapid progress which has been made in the development of new dyes and molecular markers which bind to specific molecular targets. Rapid growth in this area is

likely to continue both for fundamental scientific research and as mechanisms for evaluating new therapies. Optical imaging is well placed to form an intrinsic role in molecular imaging especially with the availability of novel, specifically targeted, efficient molecular beacons. In particular, quantum dots can act as highly efficient fluorophores whose optical and biochemical characteristics can be finely controlled (Salata 2004, Kim *et al* 2004). New femtosecond laser sources and faster detectors (Steinmeyer 2003) may lead to optical imaging systems designed specifically for small animal imaging.

5.2. Modelling and reconstruction

The growth in the use of prior information for both modelling and the inverse problem can be expected to continue. Simultaneous recording of anatomical and optical data for both breast and brain imaging will provide knowledge of the internal and external geometry of the tissue, as well as the precise locations of the source and detector fibres, leading to more accurate forward models. If the location of a breast lesion can be identified by anatomical imaging, the functional parameters can then be determined optically. The first steps towards this approach have been taken by Ntziachristos *et al* (2002c), Brooksby *et al* (2003) and Li *et al* (2003). The use of prior information for brain imaging is less well developed, but could be expected to provide even greater improvement in image quality than for breast imaging. An MRI image of the head can provide the location of the non-scattering regions, allowing these to be modelled correctly, possibly by using a coupled radiosity-diffusion model. Furthermore, diffusion tensor imaging can provide information about the direction of the anisotropic scatter of brain tissue. Over the next few years we can expect to see similar advances in the use of prior information in the inverse problem, as theoretical techniques improve along with computer processing power. One promising approach is to use Bayesian techniques to generate not a single image, but a series of images which give the entire posterior probability, which takes into account both measurement and image covariances. An alternative approach might be to address the clinical issue directly and appreciate that it is not always necessary to solve the ill-posed and underdetermined imaging problem. For example, the clinical question may be ‘is this lesion a tumour?’, or even ‘is the left side of the neonatal brain different from the right side?’. The answer to such questions may be a single estimate of probability (or a 95% confidence range) and the solution may then become overdetermined and less ill-posed.

The problems of creating good quality finite element meshes which incorporate high-resolution anatomical prior information, whilst still being sparse enough to be solved efficiently in the inverse problem, remain to be solved. We can expect to see further developments in meshing techniques such as adaptive mesh refinement to optimize the performance of a finite element mesh. Multigrid methods, which vary the coarseness of the mesh as the reconstruction proceeds, have been shown to reduce computation time and improve image quality (Ye *et al* 2001) and are likely to become more widely used.

Traditional algorithms for non-linear image reconstruction, such as those discussed in section 3.4, are generally based on iteratively minimizing a cost function. This type of approach is slow because the forward problem must be solved repeatedly, and an updated distribution of optical properties must be found at each step. Recently, the first direct non-linear reconstruction techniques have been implemented in EIT (Siltanen *et al* 2000) based on a proof by Nachman (1996) in which the non-linear reconstruction problem was transformed to two linear integral equations. Mueller *et al* (2002) applied the method to a realistic simulation, and Isaacson *et al* (2004) reconstructed data acquired on an anatomically realistic phantom. In both cases, the method gave qualitatively and quantitatively accurate results. In its current form, there are disadvantages: it has not yet been shown how to extend the method to optical

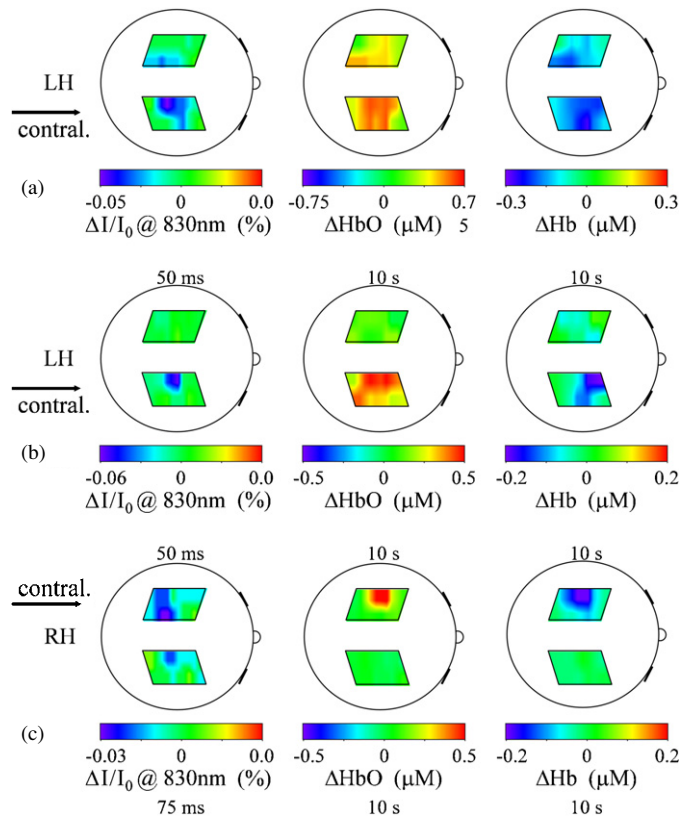


Figure 7. Optical topography images (reprinted from Franceschini and Boas (2004), with permission from Elsevier) of the fast neuronal signal 50–75 ms after onset of stimulus are shown in the left hand column, along with the corresponding oxy-haemoglobin (centre) and deoxy-haemoglobin (right) maps after 10 s of stimulation. (a) Left hand finger tapping; (b) left hand finger-tactile stimulation; (c) right hand finger-tactile stimulation.

tomography, how it can be extended to 3D, or how prior information can be included. Other approaches to direct reconstruction have been suggested in EIT (Lionheart 2004) and it is likely that these potentially important new developments will eventually be applied to diffuse optical reconstruction.

5.3. Clinical applications

The use of NIR techniques to image haemodynamic changes is now well established. In neurophysiological terms, however, the electrical activity of neurones is of primary interest and the haemodynamic response is a secondary effect. However, optical techniques have already been used to examine neuronal activity in cell cultures (Cohen 1973, Lazebnik *et al* 2003) and in the exposed brain (Rector *et al* 2001). This small, fast signal has been recorded noninvasively in humans by Gratton *et al* (1997) and Gratton and Fabiani (2003) using a frequency-domain system (ISS Inc., USA) and was shown to correlate temporally with EEG and spatially with the haemodynamic response imaged by fMRI. The signal has been observed in measurements of both phase and amplitude (Wolf *et al* 2003). More recently, Franceschini and Boas (2004) used a CW system to record fast neuronal signals from approximately 60% of subjects following 1000 averaged active or passive motor repetitions (see figure 7).

The nature of the relationship between neuronal activity and the associated haemodynamic response, known as neurovascular coupling, is not well understood. This can lead to uncertainties in the interpretation of brain imaging techniques which are sensitive to haemodynamic effects. The ability of optical methods to image both phenomena simultaneously could provide a unique system for the examination of the coupling between the two effects and thereby lead to new insights into brain physiology (Lauritzen and Gold 2003). This could have particular advantages for the assessment of brain development in infants and for the investigation of certain neurological conditions. For example, epilepsy may be initiated by pathological neuronal activity in deeper brain structures which later propagates to the cortex where it manifests as an increase in blood flow. Optical tomography may be able to localize the initial focus of epilepsy, providing more accurate diagnosis and leading to improved therapy.

One of the most challenging future roles for diffuse optical imaging is 3D imaging of the newborn infant brain, which faces unique problems due to the vulnerability of the subject. In order that optical tomography of the infant brain can have the greatest impact on mortality and the incidence of permanent brain injury, the task over the next few years is to develop a technique which can be employed rapidly and easily at the bedside, within hours of birth. Means must also be developed for monitoring the brain over periods of hours or days in order to assess the response to new forms of treatment. In future, optical tomography may also aid the study of the healthy developing brain via the increased scatter produced by myelin, as it develops around neurones.

Optical mammography has been widely evaluated as a clinical tool. Large scale clinical trials involving 300 patients have been carried out as part of the EU funded OPTIMAMM project (section 4.3) and have identified 80–85% of tumours (Grosenick *et al* 2004a, Taroni *et al* 2004b). A new multi-centre network funded by the US National Cancer Institute is likely to lead to significant developments by bringing together groups with different areas of expertise (NTROI: www.bli.uci.edu/NTROI/indexmain.html). It is likely that the clinical utility of optical mammography will increase as more wavelengths provide improved distinction between chromophores, and full tomographic reconstruction improves spatial discrimination. Furthermore, the use of optical mammography to provide functional information as an adjunct to anatomical imaging techniques is still in its infancy. The application of molecular imaging techniques to optical mammography could lead to particularly exciting clinical advances (Ntziachristos *et al* 2002a).

One aspect of optical imaging which is common to all applications is the development of improved ways to attach sources and detectors to the body. A range of approaches have been developed, from rigid arrays for mammography (Dehghani *et al* 2003b) to moulded pads for brain imaging (Hebden *et al* 2002, Koizumi *et al* 2003), and even non-contact imaging (Schulz *et al* 2003). Unwanted physiological effects can be the dominant source of error in optical imaging and so optimizing the location of the source and detector fibres and minimizing the coupling effects can lead to significant improvements in image quality (Strangman *et al* 2003, Franceschini and Boas 2004).

6. Conclusion

The field of diffuse optical imaging has made significant advances since the two reviews of 'optical imaging in medicine' were published in *Physics in Medicine and Biology* in 1997. Imaging systems have become faster, more robust, less susceptible to error, and able to acquire data with more source–detector combinations and at more wavelengths. Images are now routinely reconstructed in 3D, using more sophisticated techniques which can be adapted

to the clinical situation by incorporating prior information and by compensating for some of the unavoidable sources of measurement error. The greatest recent progress has probably been in the demonstration of clinical applications: many hundreds of optical breast and brain examinations have now been carried out worldwide.

However, diffuse optical imaging is still primarily a laboratory-based technique and has yet to progress to routine clinical use. Improvements are still required in qualitative and quantitative accuracy, both of which are limited by poor spatial resolution. Recent developments, in particular the use of anatomical prior information, are already indicating that improved image quality is achievable. It seems increasingly probable that optical techniques could play a major clinical role when used as adjuncts to other imaging systems. For example, the addition of an integrated optical imaging system to a new MR imaging facility may provide enhanced clinical information about haemodynamics and metabolism at minimal additional cost and complexity compared to the MRI system itself.

A further role which optical imaging could fill is as a low-cost, portable imaging system for use in primary care situations or at the bedside. Similarly, optical imaging has already led to increased knowledge of brain physiology when used by psychology researchers who may not have access to an expensive fMRI system, and it can provide unique information about neurovascular coupling and brain development.

The transfer of new techniques and ideas for diffuse optical imaging into clinical tools remains a demanding problem, requiring close collaboration between engineers, clinicians, scientists and mathematicians. We will only know what clinical utility diffuse optical imaging can ultimately have when the ideal instrumentation is combined with the best modelling and reconstruction methods, and applied to the most appropriate clinical question.

References

- Araraki L S L, Ntziachristos V, Chance B, Leigh J S and Schotland J C 2000 Optical diffusion tomography of the exercising human forearm *OSA Biomedical Topical Meetings (Miami)* pp 374–7
- Arridge S R 1995 Photon measurement density functions: I. Analytical forms *Appl. Opt.* **34** 7395–409
- Arridge S R 1999 Optical tomography in medical imaging *Inverse Problems* **15** R41–R93
- Arridge S R, Cope M and Delpy D T 1992 The theoretical basis for the determination of optical pathlengths in tissue: temporal and frequency analysis *Phys. Med. Biol.* **37** 1531–59
- Arridge S R, Dehghani H, Schweiger M and Okada E 2000a The finite element model for the propagation of light in scattering media: a direct method for domains with nonscattering regions *Med. Phys.* **27** 252–64
- Arridge S R and Hebden J C 1997 Optical imaging in medicine: II. Modelling and reconstruction *Phys. Med. Biol.* **42** 841–53
- Arridge S R, Hebden J C, Schweiger M, Schmidt F E W, Fry M E, Hillman E M C, Dehghani H and Delpy D T 2000b A method for 3D time-resolved optical tomography *Int. J. Imaging Syst. Technol.* **11** 2–11
- Arridge S R and Lionheart W R B 1998 Nonuniqueness in diffusion-based optical tomography *Opt. Lett.* **23** 882–4
- Arridge S R and Schweiger M 1995 Photon measurement density functions: II. Finite element method calculations *Appl. Opt.* **34** 8026–37
- Arridge S R, Schweiger M, Hiraoka M and Delpy D T 1993 Finite element approach for modelling photon transport in tissue *Med. Phys.* **20** 299–309
- Aydin E D, de Oliveira C R E and Goddard A J H 2002 A comparison between transport and diffusion calculations using a finite element-spherical harmonics radiation transport method *Med. Phys.* **29** 2013–23
- Bagshaw A P, Liston A D, Bayford R H, Tizzard A, Gibson A P, Tidswell A T, Sparkes M K, Dehghani H, Binnie C D and Holder D S 2003 Electrical impedance tomography of human brain function using reconstruction algorithms based on the finite element method *Neuroimage* **20** 752–63
- Banks E *et al* 2004 Influence of personal characteristics of individual women on sensitivity and specificity of mammography in the Million Women Study: cohort study *Br. Med.J.* **329** 477–82
- Barbour R L, Graber H, Pei Y, Zhong S and Schmitz C H 2001 Optical tomographic imaging of dynamic features of dense-scattering media *J. Opt. Soc. Am. A* **18** 3018–36

- Barbour R L, Schmitz C H, Klemer D P, Pei Y and Graber H L 2004 Design and initial testing of system for simultaneous bilateral dynamic optical tomographic mammography *OSA Biomedical Topical Meetings (Miami) WD4*
- Barnett A H, Culver J P, Sorensen A G, Dale A and Boas D A 2003 Robust inference of baseline optical properties of the human head with three-dimensional segmentation from magnetic resonance imaging *Appl. Opt.* **42** 3095–108
- Bayford R H, Gibson A P, Tizzard A, Tidswell T and Holder D S 2001 Solving the forward problem in electrical impedance tomography for the human head using IDEAS (integrated design engineering analysis software), a finite element modelling tool *Physiol. Meas.* **22** 55–64
- Benaron D A *et al* 2000 Noninvasive functional imaging of human brain using light *J. Cereb. Blood Flow Metab.* **20** 469–77
- Benaron D A, Ho D C, Spilman S D, van Houten J C and Stevenson D K 1994a Non-recursive linear algorithms for optical imaging in diffusive media *Adv. Exp. Med. Biol.* **361** 215–22
- Benaron D A, Ho D C, Spilman S D, van Houten J C and Stevenson D K 1994b Tomographic time-of-flight optical imaging device *Adv. Exp. Med. Biol.* **361** 207–14
- Blarney R W, Wilson A R M and Patnick J 2000 Screening for breast cancer *Br. Med. J.* **321** 689–93
- Bluestone A Y, Abdouleav G, Schmitz C H, Barbour R L and Hielscher A H 2001 Three-dimensional optical tomography of hemodynamics in the human head *Opt. Express* **9** 272–86
- Boas D A, Brooks D H, Miller E L, DiMarzio C A, Kilmer M, Gaudette R J and Zhang Q 2001a Imaging the body with diffuse optical tomography *IEEE Signal Process. Mag.* **18** 57–75
- Boas D A, Chen K, Grebert D and Franceschini M A 2004b Improving the diffuse optical imaging spatial resolution of the cerebral hemodynamic response to brain activation in humans *Opt. Lett.* **29** 1506–8
- Boas D A, Culver J P, Stott J J and Dunn A K 2002 Three dimensional Monte Carlo code for photon migration through complex heterogeneous media including the adult human head *Opt. Express* **10** 159–69
- Boas D A, Dale A M and Franceschini M A 2004a Diffuse optical imaging of brain activation: approaches to optimizing image sensitivity, resolution and accuracy *Neuroimage* **23** 275–88
- Boas D A, Gaudette T and Arridge S R 2001b Simultaneous imaging and optode calibration with diffuse optical tomography *Opt. Express* **8** 263–70
- Boas D A, Gaudette T, Strangman G, Cheng X, Marota J J and Mandeville J B 2001c The accuracy of near infrared spectroscopy and imaging during focal changes in cerebral hemodynamics *Neuroimage* **13** 76–90
- Boas D A, O'Leary M A, Chance B and Yodh A G 1994 Scattering of diffuse photon density waves by spherical inhomogeneities within turbid media: analytic solution and applications *Proc. Natl Acad. Sci. USA* **91** 4887–91
- Boppart S A 2003 Optical coherence tomography: technology and applications for neuroimaging *Psychophysiology* **40** 529–41
- Borcea L 2002 Electrical impedance tomography *Inverse Problems* **18** R99–R136
- Borsic A 2002 Regularisation methods for imaging from electrical measurements *PhD Thesis* Oxford Brookes University
- Bright R 1831 *Diseases of the Brain and Nervous System* vol 2431 (London: Longman)
- Brooksby B, Dehghani H, Pogue B W and Paulsen K D 2003 Near infrared (NIR) tomography breast image reconstruction with a priori structural information from MRI: algorithm development for reconstructing heterogeneities *IEEE J. Quantum Electron.* **9** 199–209
- Carminati R, Elaloufi R and Greffet J-J 2004 Beyond the diffusing-wave spectroscopy model for the temporal fluctuations of scattered light *Phys. Rev. Lett.* **92** 213904-1-213904-4
- Cerussi A E, Berger A J, Bevilacqua F, Shah N, Jakubowski D, Butler J, Holcombe R F and Tromberg B J 2001 Sources of absorption and scattering contrast for near infrared optical mammography *Acad. Radiol.* **8** 211–8
- Chance B *et al* 1998a A novel method for fast imaging of brain function, non-invasively, with light *Opt. Express* **2** 411–23
- Chance B, Cope M, Gratton E, Ramirez N and Tromberg B J 1998b Phase measurement of light absorption and scatter in human tissue *Rev. Sci. Instrum.* **69** 3457–81
- Chernomordik V, Hattery D W, Gandjbakhche A H, Pifferi A, Taroni P, Torricelli A, Valentini G and Cubeddu R 2000 Quantification by random walk of the optical parameters of nonlocalized abnormalities embedded within tissuelike phantoms *Opt. Lett.* **25** 951–3
- Chernomordik V, Hattery D W, Gannot I, Zaccanti G and Gandjbakhche A H 2002a Analytical calculation of the mean time spent by photons inside an absorptive inclusion embedded in a highly scattering medium *J. Biomed. Opt.* **7** 486–92
- Chernomordik V, Hattery D W, Grosenick D, Wabnitz H, Rinneberg H, Moesta K T, Schlag P M and Gandjbakhche A H 2002b Quantification of optical properties of a breast tumour using random walk theory *J. Biomed. Opt.* **7** 80–7
- Cherry S R 2004 *In vivo* molecular and genomic imaging: new challenges for imaging physics *Phys. Med. Biol.* **49** R13–R48

- Cohen L B 1973 Changes in neuron structure during action potential propagation and synaptic transmission *Physiol. Rev.* **53** 373–418
- Colak S B, van der Mark M B, Hooft G W, Hoogenraad J H, van der Linden E S and Kuijpers F A 1999 Clinical optical tomography and NIR spectroscopy for breast cancer detection *IEEE J. Quantum Electron.* **5** 1143–58
- Comtat C, Hinahan P E, Fessler J A, Beyer T, Townsens D W, Defrise M and Michel C 2002 Clinically feasible reconstruction of 3D whole-body PET/CT data using blurred anatomical labels *Phys. Med. Biol.* **47** 1–20
- Cope M 1991 The application of near infrared spectroscopy to non invasive monitoring of cerebral oxygenation in the newborn infant *PhD thesis* University of London
- Corlu A, Durduran T, Choe R, Schweiger M, Hillman E M C, Arridge S R and Yodh A G 2003 Uniqueness and wavelength optimization in continuous-wave multispectral diffuse optical tomography *Opt. Lett.* **28** 2339–431
- Cubeddu R, Comelli D, D'Andrea C, Taroni P and Valentini G 2002 Time-resolved fluorescence imaging in biology and medicine *J. Phys. D: Appl. Phys.* **35** R61–R76
- Culver J P, Choe R, Holboke M J, Zubkov L, Durduran T, Slemp A, Ntziachristos V, Chance B and Yodh A G 2003a Three-dimensional diffuse optical tomography in the parallel plane transmission geometry: evaluation of a hybrid frequency domain/continuous wave clinical system for breast imaging *Med. Phys.* **30** 235–47
- Culver J P, Durduran T, Furuya D, Cheung C, Greenberg J H and Yodh A G 2003b Diffuse optical tomography of cerebral blood flow, oxygenation and metabolism in rat during focal ischaemia *J. Cereb. Blood Flow Metab.* **23** 911–24
- Culver J P, Siegel A M, Stott J J and Boas D A 2003c Volumetric diffuse optical tomography of brain activity *Opt. Lett.* **28** 2061–3
- Curling T B 1843 *A Practical Treatise on the Diseases of the Testis and of the Spermatic Cord and Scrotum* (London: Samuel Highley) pp 125–81
- Cutler M 1929 Transillumination as an aid in the diagnosis of breast lesions *Surg. Gynecol. Obstet.* **48** 721–8
- Dagdug L, Weiss G H and Gandjbakhche A H 2003 Effects of anisotropic optical properties on photon migration in structured tissues *Phys. Med. Biol.* **48** 1361–70
- Danen R M, Wang Y, Li X D, Thayer W S and Yodh A G 1998 Regional imager for low resolution functional imaging of the brain with diffusing near-infrared light *Photochem. Photobiol.* **67** 33–40
- Dehghani H, Brooksby B, Vishwanath K, Pogue B W and Paulsen K D 2003a The effect of internal refractive index variation on near-infrared optical tomography: a finite element modelling approach *Phys. Med. Biol.* **48** 2713–27
- Dehghani H, Doyley M M, Pogue B W, Jiang S, Geng J and Paulsen K D 2004 Breast deformation modelling for image reconstruction in near infrared optical tomography *Phys. Med. Biol.* **49** 1131–45
- Dehghani H, Pogue B W, Poplack S P and Paulsen K D 2003b Multiwavelength three-dimensional near-infrared tomography of the breast: initial simulation, phantom and clinical results *Appl. Opt.* **42** 135–45
- Dorn O 1998 A transport-backtransport method for optical tomography *Inverse Problems* **14** 1107–30
- Dorn O 2002 Shape reconstruction in scattering media with voids using a transport model and level sets *Can. Appl. Math. Q.* **10** 239–76
- Dunsby C and French P M W 2003 Techniques for depth-resolved imaging through turbid media including coherence gated imaging *J. Phys. D: Appl. Phys.* **36** R207–R227
- Durduran T, Choe R, Culver J P, Zubkov L, Holboke M J, Giammarco J, Chance B and Yodh A G 2002 Bulk optical properties of healthy female breast tissue *Phys. Med. Biol.* **47** 2847–61
- Eda H *et al* 1999 Multichannel time-resolved optical tomographic imaging system *Rev. Sci. Instrum.* **70** 3595–602
- Eppstein M J, Dougherty D E, Hawrysz D J and Sevick-Muraca E M 2001 Three-dimensional Bayesian optical image reconstruction with domain decomposition *IEEE Trans. Med. Imaging* **20** 147–63
- Eppstein M J, Hawrysz D J, Godavarty A and Sevick-Muraca E M 2002 Three-dimensional, Bayesian image reconstruction from sparse and noisy data sets: near-infrared fluorescence tomography *Proc. Natl Acad. Sci.* **99** 9619–24
- Evans S N and Stark P B 2002 Inverse problems as statistics *Inverse Problems* **18** R55–R97
- Everdell N, Gibson A P, Tullis I D C, Vaithianathan T, Hebden J and Delpy D T 2004 A frequency multiplexed near infra-red topography system for imaging functional activation in the brain *OSA Biomedical Topical Meetings (Miami)* WF33
- Fantini S, Walker S A, Franceschini M A, Kaschke M, Schlag P M and Moesta K T 1998 Assessment of the size, position and optical properties of breast tumors in vivo by noninvasive optical methods *Appl. Opt.* **37** 1982–9
- Fercher A F, Drexler W, Hitzenberger C W and Lasser T 2003 Optical coherence tomography—principles and applications *Rep. Prog. Phys.* **66** 239–303
- Ferlay J, Bray F, Pisani P and Parkin D M 2001 GLOBOCAN 2000: cancer incidence, mortality and prevalence worldwide, version 1.0 *IARC CancerBase* no 5
- Ferrari M, Mottola L and Quaresima V 2004 Principles, techniques, and limitations of near infrared spectroscopy *Can. J. Appl. Physiol.* **29** 463–87

- Ferwerda H A 1999 The radiative transfer equation for scattering media with a spatially varying refractive index *J. Opt. A: Pure Appl. Opt.* **1** L1–L2
- Fletcher S W and Elmore J G 2003 Mammographic screening for breast cancer *N Engl J. Med.* **348** 1672–80
- Franceschini M A and Boas D A 2004 Noninvasive measurement of neuronal activity with near-infrared optical imaging *Neuroimage* **21** 372–86
- Franceschini M A, Fantini S, Thompson J H, Culver J P and Boas D A 2003 Hemodynamic evoked response of the sensorimotor cortex measured noninvasively with near-infrared optical imaging *Psychophysiology* **40** 548–560
- Franceschini M A, Moesta K T, Fantini S, Gaida G, Gratton E, Jess H, Mantulin W W, Seeber M, Schlag P M and Kaschke M 1997 Frequency-domain techniques enhance optical mammography: initial clinical results *Proc. Natl Acad. Sci. USA* **94** 6468–73
- Franceschini M A, Toronov V, Filiaci M E, Gratton E and Fantini S 2000 On-line optical imaging of the human brain with 160 ms temporal resolution *Opt. Express* **6** 49–57
- Fujimoto J G 2003 Optical coherence tomography for ultrahigh resolution in vivo imaging *Nature Biotech.* **21** 1361–7
- Gaudette R J, Brooks D H, DiMarzio C A, Kilmer M, Miller E L, Gaudette T and Boas D A 2000 A comparison study of linear reconstruction techniques for diffuse optical tomographic imaging of absorption coefficient *Phys. Med. Biol.* **45** 1051–70
- Gibson A P, Riley J, Schweiger M, Hebden J C, Arridge S R and Delpy D T 2003 A method for generating patient-specific finite element meshes for head modelling *Phys. Med. Biol.* **48** 481–95
- Godovarty A, Thompson A B, Roy R, Gurfinkel M, Eppstein M, Zhang C and Sevick-Muraca E M 2004 Diagnostic imaging of breast cancer using fluorescence-enhanced optical tomography: phantom studies *J. Biomed. Opt.* **9** 488–96
- Goertzen A L, Meadors A K, Silverman R W and Cherry S R 2002 Simultaneous molecular and anatomical imaging of the mouse *in vivo* *Phys. Med. Biol.* **47** 4315–28
- Götz L, Heywang-Köbrunner S H, Schütz O and Siebold H 1998 Optische mammographie an praoperativen patientinnen *Akt. Radiol.* **8** 31–3
- Graber H, Pei Y and Barbour R L 2002 Imaging of spatiotemporal coincident states by DC optical tomography *IEEE Trans. Med. Imaging* **21** 852–66
- Graber H L, Zhong S, Pei Y, Arif I, Hira J and Barbour R L 2000 Dynamic imaging of muscle activity by optical tomography *Biomedical Topical Meetings, OSA Technical Digest (OSA, Washington DC)* pp 407–8
- Grable R J, Rohler D P and Sastry K L A 2004 Optical tomography breast imaging *Proc. SPIE* **2979** 197–210
- Gratton G, Corballis P M, Cho E, Fabiani M and Hood D C 1995 Shades of grey matter: noninvasive optical images of human brain responses during visual stimulation *Psychophysiology* **32** 505–9
- Gratton G and Fabiani M 2003 The event-related optical signal (EROS) in visual cortex: replicability, consistency, localization and resolution *Psychophysiology* **40** 561–71
- Gratton G, Fabiani M, Corballis P M, Hood D C, Goodman-Wood M R, Hirsch J, Kim K, Friedman D and Gratton E 1997 Fast and localized event-related optical signals (EROS) in the human occipital cortex: comparisons with the visual evoked potential and fMRI *Neuroimage* **6** 168–80
- Grosenick D, Moesta K T, Wabnitz H, Mucke J, Möller M, Stössel J, Wassermann B, Macdonald R, Schlag P M and Rinneberg H 2004a Time domain optical mammography on 150 patients: hemoglobin concentration and blood oxygen saturation of breast tumours *OSA Biomedical Topical Meetings (Miami) ThB2*
- Grosenick D, Moesta K T, Wabnitz H, Mucke J, Stroszczyński C, Macdonald R, Schlag P M and Rinneberg H 2003 Time-domain optical mammography: initial clinical results on detection and characterization of breast tumors *Appl. Opt.* **42** 3170–86
- Grosenick D, Wabnitz H, Moesta K T, Mucke J, Möller M, Stroszczyński C, Stössel J, Wassermann B, Schlag P M and Rinneberg H 2004b Concentration and oxygen saturation of haemoglobin of 50 breast tumours determined by time-domain optical mammography *Phys. Med. Biol.* **49** 1165–81
- Grosenick D, Wabnitz H, Rinneberg H H, Moesta K T and Schlag P M 1999 Development of a time-domain optical mammograph and first in vivo applications *Appl. Opt.* **38** 2927–43
- Hampel U and Freyer R 1998 Fast image reconstruction for optical absorption tomography in media with radially symmetric boundaries *Med. Phys.* **25** 92–101
- Hawrysz D J and Sevick-Muraca E M 2000 Developments towards diagnostic breast cancer imaging using near-infrared optical measurements and fluorescent contrast agents *Neoplasia* **2** 388–417
- Hayashi T, Kashio Y and Okada E 2003 Hybrid Monte Carlo-diffusion method for light propagation in tissue with a low-scattering region *Appl. Opt.* **42** 2888–96
- Hebden J C 2003 Advances in optical imaging of the newborn infant brain *Psychophysiology* **40** 501–10
- Hebden J C, Arridge S R and Delpy D T 1997 Optical imaging in medicine: I. Experimental techniques *Phys. Med. Biol.* **42** 825–40
- Hebden J C and Delpy D T 1994 Enhanced time resolved imaging using a diffusion model of photon transport *Opt. Lett.* **19** 311–3

- Hebden J C and Delpy D T 1997 Diagnostic imaging with light *Br. J. Radiol.* **70** S206–S214
- Hebden J C, Garcia Guerrero J J, Chernomordik V and Gandjbakhche A H 2004a Experimental evaluation of an anisotropic scattering model of a slab geometry *Opt. Lett.* **29** 2518–20
- Hebden J C, Gibson A P, Austin T, Yusof R M, Everdell N, Delpy D T, Arridge S R, Meek J H and Wyatt J S 2004b Imaging changes in blood volume and oxygenation in the newborn infant brain using three-dimensional optical tomography *Phys. Med. Biol.* **49** 1117–30
- Hebden J C, Gibson A P, Yusof R M, Everdell N, Hillman E M, Delpy D T, Austin T, Meek J and Wyatt J S 2002 Three-dimensional optical tomography of the premature infant brain *Phys. Med. Biol.* **47** 4155–66
- Hebden J C, Kruger R A and Wong K S 1991 Time resolved imaging through a highly scattering medium *Appl. Opt.* **30** 788–94
- Heino J, Arridge S R, Sikora J and Somersalo E 2003 Anisotropic effects in highly scattering media *Phys. Rev. E* **68** 031908
- Heino J and Somersalo E 2002 Estimation of optical absorption in anisotropic background *Inverse Problems* **18** 559–73
- Hielscher A H, Klose A D and Hanson K M 1999 Gradient-based iterative image reconstruction scheme for time-resolved optical tomography *IEEE Trans. Med. Imaging* **18** 262–71
- Hielscher A H, Klose A D, Scheel A K, Moa-Anderson B, Backhaus M, Netz U and Beuthan J 2004 Sagittal laser optical tomography for imaging of rheumatoid finger joints *Phys. Med. Biol.* **49** 1147–63
- Hillman E M C, Boas D A, Dale A M and Dunn A K 2004 Lamellar optical tomography: demonstration of millimetre-scale depth-resolved imaging in turbid media *Opt. Lett.* **29** 1650–2
- Hillman E M C, Hebden J C, Schmidt F E W, Arridge S R, Schweiger M, Dehghani H and Delpy D T 2000 Calibration techniques and datatype extraction for time-resolved optical tomography *Rev. Sci. Instrum.* **71** 3415–27
- Hillman E M C, Hebden J C, Schweiger M, Dehghani H, Schmidt F E, Delpy D T and Arridge S R 2001 Time resolved optical tomography of the human forearm *Phys. Med. Biol.* **46** 1117–30
- Hintz S R, Benaron D A, Siegel A M, Zourabian A, Stevenson D K and Boas D A 2001 Bedside functional imaging of the premature infant brain during passive motor activation *J. Perinat. Med.* **29** 335–43
- Hintz S R, Benaron D A, van Houten J P, Duckworth J L, Liu F W H, Spilman S D, Stevenson D K and Cheong W-F 1998 Stationary headband for clinical time-of-flight optical imaging at the bedside *Photochem. Photobiol.* **68** 361–9
- Hintz S R, Cheong W F, van Houten J P, Stevenson D K and Benaron D A 1999 Bedside imaging of intracranial hemorrhage in the neonate using light: comparison with ultrasound, computed tomography, and magnetic resonance imaging *Pediatr. Res.* **45** 54–9
- Hoenders B J 1997 Existence of invisible nonscattering objects and nonradiating sources *J. Opt. Soc. Am. A* **14** 262–6
- Holboke M J, Tromberg B J, Li X, Shah N, Fishkin J B, Kidney D, Butler J, Chance B and Yodh A G 2000 Three-dimensional diffuse optical mammography with ultrasound localization in a human subject *J. Biomed. Opt.* **5** 237–47
- Hoshi Y 2003 Functional near-infrared optical imaging: utility and limitations in human brain mapping *Psychophysiology* **40** 511–20
- Houssami N, Irwig L, Simpson J M, McKessar M, Blome S and Noakes J 2004 The influence of clinical information on the accuracy of diagnostic mammography *Breast Cancer Res. Treat.* **85** 223–8
- Intes X, Ripoll J, Chen Y, Nioka S, Yodh A G and Chance B 2003 In vivo continuous-wave optical breast imaging enhanced with Indocyanine Green *Med. Phys.* **30** 1039–47
- Isaacson D, Mueller J L, Newell J C and Siltanen S 2004 Reconstructions of chest phantoms by the D-bar method for electrical impedance tomography *IEEE Trans. Med. Imaging* **23** 821–8
- Isakov V 1993 Uniqueness and stability in multi-dimensional inverse problems *Inverse Problems* **9** 579–621
- Jiang H, Ifimia N V, Xu Y, Eggert J A, Fajardo L L and Klove K L 2002 Near-infrared optical imaging of the breast with model-based reconstruction *Acad. Radiol.* **9** 186–94
- Joshi A, Thompson A B, Sevick-Muraca E M and Bangerth W 2004 Adaptive finite element methods for forward modelling in fluorescence enhanced frequency domain optical tomography *OSA Biomedical Topical Meetings (Miami)* WB7
- Kaipio J P, Kolehmainen V, Somersalo E and Vauhkonen M 2000 Statistical inversion and Monte Carlo sampling methods in electrical impedance tomography *Inverse Problems* **16** 1487–522
- Kaipio J P, Kolehmainen V, Vauhkonen M and Somersalo E 1999 Inverse problems with structural prior information *Inverse Problems* **15** 713–29
- Kaschke M, Jess H, Gaida G, Kaltenbach J-M and Wrobel W 1994 Transillumination imaging of tissue by phase modulation techniques *Proc. OSA Advances in Optical Imaging and Photon Migration* vol 21 pp 88–92
- Kawasaki S, Kawaguchi F and Ichikawa N 2002 Optical topography image mapping on 3-dimensional brain surface *Neuroimage Human Brain Mapping Meeting*

- Kilmer M, Miller E L, Barbaro A and Boas D A 2003 Three-dimensional shape-based imaging of absorption perturbation for diffuse optical tomography *Appl. Opt.* **42** 3129–44
- Kim A 2004 Transport theory for light propagation in biological tissue *J. Opt. Soc. Am. A* **21** 820–7
- Kim S *et al* 2004 Near-infrared fluorescent type II quantum dots for sentinel lymph node mapping *Nature Biotechnol.* **22** 93–7
- Kim A D and Ishimaru A 1998 Optical diffusion of continuous-wave, pulsed and density waves in scattering media and comparisons with radiative transfer *Appl. Opt.* **37** 5313–9
- Kim A and Keller J B 2003 Light propagation in biological tissue *J. Opt. Soc. Am. A* **20** 92–8
- Klose A D and Hielscher A H 1999 Iterative reconstruction scheme for optical tomography based on the equation of radiative transfer *Med. Phys.* **28** 1698–707
- Klose A D and Hielscher A H 2003 Fluorescence tomography with simulated data based on the equation of radiative transfer *Opt. Lett.* **28** 1019–21
- Klose A D, Ntziachristos V and Hielscher A H 2004 Experimental validation of a fluorescence tomography algorithm based on the equation of radiative transfer *OSA Biomedical Topical Meetings (Miami)* SA6
- Knoll G F 1999 Radiation detection and measurement *Wiley Text Books* 3rd edn (New York: Wiley)
- Kohlemainen V 2001 Novel approaches to image reconstruction in diffusion tomography *PhD Thesis* University of Kuopio
- Kohlemainen V, Arridge S R, Lionheart W R B, Vauhkonen M and Kaipio J P 1999 Recovery of region boundaries of piecewise constant coefficients of an elliptic PDE from boundary data *Inverse Problems* **15** 1375–91
- Kohlemainen V, Arridge S R, Vauhkonen M and Kaipio J P 2000a Simultaneous reconstruction of internal tissue region boundaries and coefficients in optical diffusion tomography *Phys. Med. Biol.* **45** 3267–83
- Kohlemainen V, Prince S, Arridge S R and Kaipio J P 2003 State-estimation approach to the nonstationary optical tomography problem *J. Opt. Soc. Am. A* **20** 876–89
- Kohlemainen V, Vauhkonen M, Kaipio J P and Arridge S R 2000b Recovery of piecewise constant coefficients in optical diffusion tomography *Opt. Express* **7** 468–80
- Koizumi H, Yamamoto T, Maki A, Yamashita Y, Sato H, Kawaguchi H and Ichikawa N 2003 Optical topography: practical problems and new applications *Appl. Opt.* **42** 3054–62
- Kusaka T, Kawada K, Okubo K, Nagano K, Namba M, Okada H, Imai T, Isobe K and Itoh S 2004 Noninvasive optical imaging in the visual cortex in young infants *Hum. Brain Mapp.* **22** 122–32
- Kwee I 1999 Towards a Bayesian framework for optical tomography *PhD Thesis* University of London
- Lauritzen M and Gold L 2003 Brain function and neurophysiological correlates of signals used in functional neuroimaging *J. Neurosci.* **23** 3972–80
- Lazebnik M, Marks D L, Potieter K, Gillette R and Boppart S A 2003 Functional optical coherence tomography for detecting neural activity through scattering changes *Opt. Lett.* **28** 1218–20
- Le Bihan D, Mangin J-F, Poupon C, Clark C A, Pappata S, Molko N and Chabriat H 2001 Diffusion tensor imaging: concepts and applications *J. Magn. Reson. Imaging* **13** 534–46
- Li A *et al* 2003 Tomographic optical breast imaging guided by three-dimensional mammography *Appl. Opt.* **42** 5181–90
- Li J, Ku G and Wang L V 2002 Ultrasound-modulated optical tomography of biological tissue by use of laser speckles *Appl. Opt.* **41** 6030–5
- Li A, Zhang Q, Culver J P, Miller E L and Boas D A 2004 Reconstructing chromophore concentration images directly by continuous wave diffuse optical tomography *Opt. Lett.* **29** 256–8
- Lionheart W R B 2004 EIT reconstruction algorithms: pitfalls, challenges and recent developments *Physiol. Meas.* **25** 125–42
- Lucassen A, Watson E and Eccles D 2004 Advice about mammography for a young woman with a family history of breast cancer *Br. Med. J.* **322** 1040–2
- Maris M, Gratton E, Maier J, Mantulin W and Chance B 1994 Functional near-infrared imaging of doxygenated hemoglobin during exercise of the finger extensor muscles using the frequency-domain technique *Bioimaging* **2** 174–83
- Markel V A 2004 Modified spherical harmonics method for solving the radiative transport equation *Waves Random Media* **14** L13–L19
- Markel V A, O'Sullivan J A and Schotland J C 2003 Inverse problem in optical diffusion tomography: IV. Nonlinear inversion formulas *J. Opt. Soc. Am. A* **20** 903–12
- Markel V A and Schotland J C 2001 Inverse problem in optical diffusion tomography: I. Fourier–Laplace inversion formulas *J. Opt. Soc. Am. A* **18** 1336–47
- Martelli F, Sassaroli A, Yamada Y and Zaccanti G 2002 Analytical approximate solutions of the time-domain diffusion equation in layered slabs *J. Opt. Soc. Am. A* **19** 71–80
- Marti-Lopez L, Bouza-Dominguez J, Hebden J C, Arridge S R and Martinez-Celirio R A 2003 Validity conditions for the radiative transfer equation *J. Opt. Soc. Am. A* **20** 2046–56

- Matcher S J 1999 Nonuniqueness in optical tomography: relevance of the P1 approximation *Opt. Lett.* **24** 1729–31
- Matsuo K *et al* 2003 Activation of the prefrontal cortex to trauma-related stimuli measured by near-infrared spectroscopy in posttraumatic stress disorder due to terrorism *Psychophysiology* **40** 492–500
- McBride T, Pogue B W, Jiang S, Osterberg U L and Paulsen K D 2001 A parallel-detection frequency-domain near-infrared tomography system for hemoglobin imaging of the breast in vivo *Rev. Sci. Instrum.* **72** 1817–24
- Metherall P, Barber D C, Smallwood R H and Brown B H 1996 Three-dimensional electrical impedance tomography *Nature* **380** 509–12
- Moesta K T, Kaisers H, Fantini S, Tönnies M, Kaschke M and Schlag P M 1996 Lasermammografie der Brustdrüse-Sensitivitätssteigerung durch Hochfrequenzmodulation *Langenbecks Arch. Chir. Suppl.* **1** 543–8
- Molinari M, Blott B H, Cox S J and Daniell G J 2002 Optimal imaging with adaptive mesh refinement in electrical impedance tomography *Physiol. Meas.* **23** 121–8
- Morris E, Liberman L, Ballon D J, Robson M, Abramson A F, Heerdt A and Dershaw D D 2003 MRI of occult breast carcinoma in a high-risk population *Am. J. Radiol.* **181** 619–26
- Mosegaard K and Sambridge M 2002 Monte Carlo analysis of inverse problems *Inverse Problems* **18** R29–R54
- Mueller J L, Siltanen S and Isaacson D 2002 A direct reconstruction algorithm for electrical impedance tomography *IEEE Trans. Med. Imaging* **21** 555–9
- Nachman A I 1996 Global uniqueness for a two-dimensional inverse problem *Ann. Math.* **143** 71–96
- Nickell S, Hermann M, Essenpreis M, Farrell T J, Krämer U and Patterson M S 2000 Anisotropy of light propagation in human skin *Phys. Med. Biol.* **45** 2873–86
- Ntziachristos V and Chance B 2001 Probing physiology and molecular function using optical imaging: applications to breast cancer *Breast Cancer Res.* **3** 41–6
- Ntziachristos V, Ma X and Chance B 1998 Time-correlated single photon counting imager for simultaneous magnetic resonance and near-infrared mammography *Rev. Sci. Instrum.* **69** 4221–33
- Ntziachristos V, Ripoll J and Weissleder R 2002a Would near infra-red fluorescence signals propagate through large human organs for clinical studies? (with errata **27** 1652) *Opt. Lett.* **27** 333–5
- Ntziachristos V, Tung C-H, Bremer C and Weissleder R 2002b Fluorescence molecular tomography resolves protease activity in vivo *Nature Med.* **8** 757–60
- Ntziachristos V, Yodh A G, Schnall M and Chance B 2000 Concurrent MRI and diffuse optical tomography of breast after indocyanine green enhancement *Proc. Natl Acad. Sci. USA* **97** 2767–72
- Ntziachristos V, Yodh A G, Schnall M and Chance B 2002c MRI-guided diffuse optical spectroscopy of malignant and benign breast lesions *Neoplasia* **4** 347–54
- Obata A, Morimoto K, Sato H, Maki A and Koizumi H 2003 Acute effects of alcohol on hemodynamic changes during visual stimulation assessed using 24-channel near-infrared spectroscopy *Psychiatry Res.: Neuroimaging* **123** 145–52
- Obrig H and Villringer A 2003 Beyond the visible—imaging the human brain with light *J. Cereb. Blood Flow Metab.* **23** 1–18
- Oh S, Milstein A B, Millane R P, Bouman C A and Webb K J 2002 Source–detector calibration in three-dimensional Bayesian optical diffusion tomography *J. Opt. Soc. Am. A* **19** 1983–93
- Okada E and Delpy D T 2003 Near-infrared light propagation in an adult head model: I. Modeling of low-level scattering in the cerebrospinal fluid layer *Appl. Opt.* **42** 2906–14
- Pei Y, Graber H L and Barbour R L 2001 Normalized-constraint algorithm for minimizing inter-parameter crosstalk in DC optical tomography *Opt. Express* **11** 97–109
- Peña M, Maki A, Kovacic D, Dehaene-Lambertz G, Koizumi H, Bouquet F and Mehler J 2003 Sounds and silence: an optical topography study of language recognition at birth *Proc. Natl Acad. Sci. USA* **100** 11702–5
- Pera V E, Heffer E L, Siebold H, Schütz O, Heywang-Köbrunner S, Götz L, Heinig A and Fantini S 2003 Spatial second-derivative image processing: an application to optical mammography to enhance the detection of breast tumours *J. Biomed. Opt.* **8** 517–24
- Peters V G, Wyman D R, Patterson M S and Frank G L 1990 Optical properties of normal and diseased human breast tissue in the visible and near infrared *Phys. Med. Biol.* **35** 1317–34
- Pifferi A, Taroni P, Torricelli A, Messina F and Cubeddu R 2003 Four-wavelength time-resolved optical mammography in the 680–980 nm range *Opt. Lett.* **28** 1138–40
- Pifferi A, Torricelli A, Taroni P, Bassi A, Chikoidze E, Giambattistelli E and Cubeddu R 2004 Optical biopsy of bone tissue: a step toward the diagnosis of bone pathologies *J. Biomed. Opt.* **9** 474–80
- Pogue B W, Giemer S, McBride T, Jiang S, Osterberg U L and Paulsen K D 2001 Three-dimensional simulation of near-infrared diffusion in tissue: boundary condition and geometry analysis for finite-element image reconstruction *Appl. Opt.* **40** 588–600

- Pogue B W, Jiang S, Deghani H, Kogel C, Soho S, Srinivasan S, Song X, Tosteson T D, Poplack S P and Paulsen K D 2004 Characterization of hemoglobin, water and NIR scattering in breast tissue: analysis of intersubject variability and menstrual cycle changes *J. Biomed. Opt.* **9** 541–52
- Pogue B W and Paulsen K D 1998 High-resolution near-infrared tomographic imaging simulations of the rat cranium by use of a priori magnetic resonance imaging structural information *Opt. Lett.* **23** 1716–8
- Poplack S P, Paulsen K D, Hartov A, Meaney P M, Pogue B W, Tosteson T D, Grove M R, Soho S and Wells W A 2004 Electromagnetic breast imaging: average tissue property values in women with negative clinical findings *Radiology* **231** 571–80
- Prince S, Kohlemainen V, Kaipio J P, Franceschini M A, Boas D A and Arridge S R 2003 Time-series estimation of biological factors in optical diffusion tomography *Phys. Med. Biol.* **48** 1491–504
- Rector D M, Rogers R F, Schwaber J S, Harper R M and George J S 2001 Scattered-light imaging in vivo tracks fast and slow processes of neurophysiological investigation *Neuroimage* **14** 977–94
- Ren K, Abdoulaev G S, Bal G and Hielscher A H 2004 Algorithm for solving the equation of radiative transfer in the frequency domain *Opt. Lett.* **29** 578–80
- Rice A and Quinn C M 2002 Angiogenesis, thrombospondin, and ductal carcinoma in situ of the breast *J. Clin. Pathol.* **55** 569–74
- Riley J, Deghani H, Schweiger M, Arridge S R, Ripoll J and Nieto-Vesperinas M 2000 3D optical tomography in the presence of void regions *Opt. Express* **7** 462–7
- Ripoll J and Ntziachristos V 2003 Iterative boundary method for diffuse optical tomography *J. Opt. Soc. Am. A* **20** 1103–10
- Ripoll J, Ntziachristos V, Carminati R and Nieto-Vesperinas M 2001 Kirchhoff approximation for diffusive waves *Phys. Rev. E* **64** 051917
- Romanov V G and He S 2000 Some uniqueness theorems for mammography-related time-domain inverse problems for the diffusion equation *Inverse Problems* **16** 447–59
- Salata O V 2004 Applications of nanoparticles in biology and medicine *J. Nanobiotechnol.* **2** (3)
- Schmitz C H *et al* 2000 Instrumentation and calibration protocol for imaging dynamic features in dense-scattering media by optical tomography *Appl. Opt.* **39** 6466–86
- Schmidt F E W, Fry M E, Hillman E M C, Hebden J C and Delpy D T 2000 A 32-channel time-resolved instrument for medical optical tomography *Rev. Sci. Instrum.* **71** 256–65
- Schmitz C H, Locker M, Lasker J M, Hielscher A H and Barbour R L 2002 Instrumentation for fast functional optical tomography *Rev. Sci. Instrum.* **73** 429–39
- Schulz R B, Ripoll J and Ntziachristos V 2003 Noncontact optical tomography of turbid media *Opt. Lett.* **28** 1701–3
- Schulz R B, Ripoll J and Ntziachristos V 2004 Experimental fluorescence tomography of tissues with noncontact measurements *IEEE Trans. Med. Imaging* **23** 492–500
- Schweiger M and Arridge S R 1999a Application of temporal filters to time-resolved data in optical tomography *Phys. Med. Biol.* **44** 1699–717
- Schweiger M and Arridge S R 1999b Optical tomographic reconstruction in a complex head model using a priori region boundary information *Phys. Med. Biol.* **44** 2703–21
- Schweiger M, Arridge S R, Hiraoka M and Delpy D T 1995 The finite element method for the propagation of light in scattering media: boundary and source conditions *Med. Phys.* **22** 1779–92
- Schweiger M, Gibson A P and Arridge S R 2003 Computational aspects of diffuse optical tomography *IEEE Comput. Sci. Eng.* (Nov/Dec) 33–41
- Seehusen D A, Reeves M M and Fomin D A 2003 Cerebrospinal fluid analysis *Am. Fam. Physician* **68** 1103–8
- Selb J, Stott J J, Franceschini M A and Boas D A 2004 Improvement of depth sensitivity to cerebral hemodynamics with a time domain system *OSA Biomedical Topical Meetings (Miami) FC3*
- Shah N, Cerussi A, Eker C, Espinoza J, Butler J, Fishkin J B, Hornung R and Tromberg B J 2001 Noninvasive functional optical spectroscopy of human breast tissue *Proc. Natl Acad. Sci. USA* **98** 4420–5
- Siegel A M, Culver J P, Mandeville J B and Boas D A 2003 Temporal comparison of functional brain imaging with diffuse optical tomography and fMRI during rat forepaw stimulation *Phys. Med. Biol.* **48** 1391–403
- Siltanen S, Mueller J L and Isaacson D 2000 An implementation of the reconstruction algorithm of A Nachman for the 2D inverse conductivity problem *Inverse Problems* **16** 681–99
- Spinelli L, Torricelli A, Pifferi A, Taroni P and Cubeddu R 2003 Experimental test of a perturbation model for time-resolved imaging in diffusive media *Appl. Opt.* **42** 3145–53
- Steinmeyer G 2003 A review of ultrafast optics and optoelectronics *J. Opt. A: Pure Appl. Opt.* **5** R1–R15
- Stott J J, Culver J P, Arridge S R and Boas D A 2003 Optode positional calibration in diffuse optical tomography *Appl. Opt.* **42** 3154–62
- Strangman G, Boas D A and Sutton J P 2002a Non-invasive neuroimaging using near-infrared light *Biol. Psychiatry* **52** 679–93

- Strangman G, Culver J P, Thompson J H and Boas D A 2002b A quantitative comparison of simultaneous BOLD fMRI and NIRS recordings during functional brain activation *Neuroimage* **17** 719–31
- Strangman G, Franceschini M A and Boas D A 2003 Factors affecting the accuracy of near-infrared spectroscopy calculations for focal changes in oxygenation parameters *Neuroimage* **18** 865–79
- Suzuki K, Yamashita Y, Ohta K, Kaneko M, Yoshida M and Chance B 1996 Quantitative measurement of optical parameters in normal breasts using time-resolved spectroscopy: in vivo results of 30 Japanese women *J. Biomed. Opt.* **1** 330–4
- Tabar L, Yen M-F, Vitak B, Chen H-H T, Smith R A and Duffy S W 2003 Mammography service screening and mortality in breast cancer patients: 20-year follow-up before and after introduction of screening *Lancet* **361** 1405–10
- Taga G, Asakawa K, Maki A, Konishi Y and Koizumi H 2003 Brain imaging in awake infants by near-infrared optical topography *Proc. Natl Acad. Sci. USA* **100** 10722–7
- Taga G, Konishi Y, Maki A, Tachibana T, Fujiwara M and Koizumi H 2000 Spontaneous oscillation of oxy- and deoxy-hemoglobin changes with a phase difference throughout the occipital cortex of newborn infants observed using non-invasive optical topography *Neurosci. Lett.* **282** 101–4
- Takahashi K *et al* 2000 Activation of the visual cortex imaged by 24-channel near-infrared spectroscopy *J. Biomed. Opt.* **5** 93–6
- Taroni P, Danesini G, Torricelli A, Pifferi A, Spinelli L and Cubeddu R 2004a Clinical trial of time-resolved scanning optical mammography at 4 wavelengths between 683 and 975 nm *J. Biomed. Opt.* **9** 464–73
- Taroni P, Pallaro L, Pifferi A, Spinelli L, Torricelli A and Cubeddu R 2004b Multi-wavelength time-resolved optical mammography *OSA Biomedical Topical Meetings (Miami)* ThB3
- Thoresen M 2000 Cooling the newborn after asphyxia—physiological and experimental background and its clinical use *Semin. Neonatol.* **5** 61–73
- Toronov V, Webb A, Choi J H, Wolf M, Michalos A, Gratton E and Hueber D 2001a Investigation of human brain hemodynamics by simultaneous near-infrared spectroscopy and functional magnetic resonance imaging *Med. Phys.* **28** 521–7
- Toronov V, Webb A, Choi J H, Wolf M, Safonova L, Wolf U and Gratton E 2001b Study of local cerebral hemodynamics by frequency-domain near-infrared spectroscopy and correlation with simultaneously acquired functional magnetic resonance imaging *Opt. Express* **9** 417–27
- Torricelli A, Spinelli L, Pifferi A, Taroni P, Cubeddu R and Danesini G M 2003 Use of a nonlinear perturbation approach for in vivo breast lesion characterization by multi-wavelength time-resolved optical mammography *Opt. Express* **11** 853–67
- Tsujimoto S, Yamamoto T, Kawaguchi H, Koizumi H and Sawaguchi T 2004 Prefrontal cortical activation associated with working memory in adults and preschool children: an event-related optical topography study *Cereb. Cortex* **14** 703–12
- Tualle J-M and Tinet E 2003 Derivation of the radiative transfer equation for scattering media with a spatially varying refractive index *Opt. Commun.* **228** 33–8
- Turner R and Jones T 2003 Techniques for imaging neuroscience *Br. Med. Bull.* **65** 3–20
- Ugryumova N, Matcher S J and Attenburrow D P 2004 Measurement of bone mineral density via light scattering *Phys. Med. Biol.* **49** 469–83
- Uludag K, Steinbrink J, Villringer A and Obrig H 2004 Separability and cross-talk: optimizing dual wavelength combinations for near-infrared spectroscopy of the adult head *Neuroimage* **22** 583–9
- Vaithianathan T, Tullis I D C, Everdell N, Leung T, Gibson A, Meek J and Delpy D T 2004 Design of a portable near infrared system for topographic imaging of the brain in babies *Rev. Sci. Instrum.* **75** 3276–83
- Vilhunen T, Kohlemainen V, Vauhkonen M, Vanne A, Kaipio J P, Gibson A P, Schweiger M and Arridge S R 2004 Computational calibration method for optical tomography *OSA Biomedical Topical Meetings (Miami)* ThD3
- Volpe J J 2001 Neurobiology of periventricular leukomalacia in the premature infant *Pediatr. Res.* **50** 553–62
- Wang L, Jacques S L and Zhao X 1995 Continuous-wave ultrasonic modulation of scattered laser light to image objects in turbid media *Opt. Lett.* **20** 629–31
- Wang X, Pang Y, Ku G, Xie X, Stoica G and Wang L V 2003 Noninvasive laser-induced photoacoustic tomography for structural and functional in vivo imaging of the brain *Nature Biotechnol.* **21** 803–6
- Warren R 2001 Screening women at high risk of breast cancer on the basis of evidence *Eur. J. Radiol.* **39** 50–9
- Warner E *et al* 2004 Comparison of breast magnetic resonance imaging, mammography and ultrasound for surveillance of women at high risk for hereditary breast cancer *J. Clin. Oncol.* **19** 3524–31
- Watanabe E, Maki A, Kawaguchi F, Takashiro K, Yamashita Y, Koizumi H and Mayanagi Y 1998 Non-invasive assessment of language dominance with near-infrared spectroscopic mapping *Neurosci. Lett.* **256** 49–52
- Watanabe E, Nagahori Y and Mayanagi Y 2002 Focus diagnosis of epilepsy using near-infrared spectroscopy *Epilepsia* **43** (Suppl. 9) 50–5

- Webb P M, Cummings M C, Bain C J and Furnival C M 2004 Changes in survival after breast cancer: improvements in diagnosis or treatment? *The Breast* **13** 7–14
- Weiss G H, Porrà J M and Masoliver J 1998 The continuous-time random walk description of photon migration on an isotropic medium *Opt. Commun.* **146** 268–76
- Weisslader R and Ntziachristos V 2003 Shedding light onto live molecular targets *Nature Med.* **9** 123–8
- West R M, Aykroyd R G, Meng S and Williams R A 2004 Markov-chain Monte Carlo techniques and spatio-temporal modelling for medical EIT *Physiol. Meas.* **25** 181–94
- Whitelaw A 2001 Intraventricular haemorrhage and post haemorrhagic hydrocephalus: pathogenesis, prevention and future interventions *Semin. Neonatol.* **6** 135–46
- Wolf M, Wolf U, Choi J H, Toronov V, Paunescu L A, Michalos A and Gratton E 2003 Fast cerebral functional signal in the 100 ms range detected in the visual cortex by frequency-domain near-infrared spectrophotometry *Psychophysiology* **40** 521–8
- Wyatt J S 2002 Applied physiology: brain metabolism following perinatal asphyxia *Curr. Paediatr.* **12** 227–31
- Xu H, Dehghani H, Pogue B W, Springett R, Paulsen K D and Dunn J F 2003 Near-infrared imaging in the small animal brain: optimization of fiber positions *J. Biomed. Opt.* **8** 102–10
- Xu Y, Gu X, Khan T and Jiang H 2002a Absorption and scattering images of heterogeneous scattering media can be simultaneously reconstructed by use of dc data *Appl. Opt.* **41** 5427–37
- Xu Y, Iftimia N V, Jiang H, Key L L and Bolster M B 2001 Imaging of in vitro and in vivo bones and joints with continuous-wave diffuse optical tomography *Opt. Express* **8** 447–51
- Xu Y, Iftimia N V, Jiang H, Key L L and Bolster M B 2002b Three-dimensional diffuse optical tomography of bones and joints *J. Biomed. Opt.* **7** 88–92
- Yamamoto T, Maki A, Kadoya T, Tanikawa Y, Yamada Y, Okada E and Koizumi H 2002 Arranging optical fibres for the spatial resolution improvement of topographical images *Phys. Med. Biol.* **47** 3429–40
- Yamashita Y, Maki A and Koizumi H 1999 Measurement system for noninvasive dynamic optical topography *J. Biomed. Opt.* **4** 414–7
- Yamashita Y, Maki A and Koizumi H 2001 Wavelength dependence of the precision of noninvasive optical measurement of oxy-, deoxy-, and total-haemoglobin concentration *Med. Phys.* **28** 1108–14
- Yates T D, Hebden J C, Gibson A P, Everdell N L, Delpy D T, Arridge S R, Douek M and Chicken W 2004 Clinical results from a 32-channel time resolved system used to image the breast *OSA Biomedical Topical Meetings (Miami)* WF18
- Ye J C, Bouman C A, Webb K J and Millane R P 2001 Nonlinear multigrid algorithms for Bayesian optical diffusion tomography *IEEE Trans. Image Process.* **10** 909–22